Numerical Weather Prediction

The Development of an Infrared Land Surface Emissivity Atlas, and its Comparison with Modis/Terra Products

Forecasting Research Technical Report No. 405

Peter Francis

email: nwp_publications@metoffice.com

THE DEVELOPMENT OF AN INFRARED LAND SURFACE EMISSIVITY ATLAS, AND ITS COMPARISON WITH MODIS/TERRA PRODUCTS

Peter N. Francis
Met Office

Change record				
Date	Version	Author / changed by	Action/comments	Approval
Nov 2002	0.1	P N Francis	Draft version for comments from RWS	-
Jan 2003	0.2	P N Francis	Draft revised following comments from RWS. Forwarded to JRE for approval to issue as FR Technical report	Approved for issue as Technical Note by JRE
Mar 2003	1.0	P N Francis	Issued as Technical Note no. 405	-

ABSTRACT

This report describes work carried out developing an atlas of infrared land surface emissivity values suitable for use with operational data assimilation systems. The basic approach taken in developing the atlas is to apply a number of different published land class emissivity spectra to global land cover classification data. To determine the senescent state for each land point, different methods of representing the annual cycle of vegetation have been investigated, using 4 years of AVHRR Pathfinder NDVI data. The derived emissivities are compared on a regional and a global scale with land surface emissivity products available as part of the "split window" land surface temperature product from the MODIS instrument on board NASA's Terra satellite. Perhaps surprisingly, the retrieved MODIS data seem to indicate little or no seasonal variation in emissivity, and the two methods where the emissivity varies throughout the seasonal cycle generally perform worse than the method where the vegetative state is assumed to be 100% green/growing throughout the year. Using the MODIS/Terra products also available for land type and NDVI, we investigate quantitatively what green/senescent split is required to provide the optimum agreement with the MODIS split-window emissivity values for each different land type. Further analysis of additional spectral emissivity measurements was required for the "snow, ice" and "urban" land classes in order to obtain acceptable agreement with the MODIS product. Finally, some comparisons are made with the MODIS "day/night" land surface emissivity products. Significant discrepancies are seen to exist between the two MODIS schemes, which serves to highlight the uncertainties still associated with our understanding of the subject.

1. INTRODUCTION

Until recently, NWP centres have not used operational (i.e. TOVS/ATOVS) infrared radiance data over land (with the exception of the stratospheric sounding channels) as the data void areas have tended to be primarily over the oceans. However, with the gradual reduction in the radiosonde coverage in certain areas, the need to assimilate satellite data over land has become more pressing. In addition to the requirements of NWP radiance assimilation, an accurate knowledge of the land surface temperature (LST) and land surface emissivity (LSE) is of importance for many applications including hydrology, NWP and climate model surface fields, and climate impact studies.

If we are going to make progress in this area, one of the subjects which must be addressed is that of identifying accurate land surface emissivities to be used in the calculation of the background radiance field for each measurement field-of-view. Although the land surface emissivity is certainly close to unity for many land surface types, the constraints on emissivity are very stringent indeed if useful information is to be extracted from the measurements, and the assumption of unit surface emissivity will simply not be good enough. For example, Wan and Dozier (1996) have estimated that, for channels in the infrared window, the surface emissivity needs to be known to within ± 0.005 in order to retrieve land surface temperature to better than ± 1 K. This report describes work carried out attempting to develop an atlas of infrared land surface emissivity values suitable for use with operational data assimilation systems. The basic approach taken in developing the atlas is to apply a number of different published land class emissivity spectra to a global land cover classification dataset.

The plan of the report is as follows. The emissivity class spectra will be described in Section 2, and the land cover classification data in Section 3. The methodology of mapping the emissivity data onto the land cover data will be described in Section 4, where some maps of derived land surface emissivity will be shown. Section 5 briefly summarises the MODIS products which are currently available, and which have been used in this report to validate the emissivities derived for the atlas. Regional and global comparisons between the derived LSE values and the MODIS products are presented in Sections 6 and 7 respectively, and some discussions and conclusions are presented in Section 8.

2. EMISSIVITY CLASS SPECTRA

The majority of the emissivity spectra used in this report to develop the LSE atlas were taken from the study of Snyder *et al.* (1998). These spectra were developed by combining laboratory measurements of component materials with some fairly simple BRDF (Bidirectional Reflectance Distribution Function) models. The laboratory measurements of thermal infrared reflectance spectra were taken from research groups based at John Hopkins University (Salisbury and D'Aria 1992, 1994, Salisbury *et al*. 1994) and University of California, Santa Barbara (Snyder *et al*. 1997) for a wide range of component materials such as green and senescent broad and needle leaves, soils, sands, rocks, snow types, ice and water. The BRDF models were based on a sphere-plane geometrical model for sparse vegetation (Li and Strahler 1992), a volumetric model for dense vegetation (Roujean *et al*. 1992) and a rough-surface specular model for water and ice (Snyder and Wan 1998). From their study, Snyder *et al*. (1998)

concluded that fourteen emissivity classes were a good balance between too many classes with similar emissivities, and too few, whereby emissivity accuracy is reduced. These fourteen classes are summarized in Table 1.

	Emissivity class name
1	Green needle forest
2	Senescent needle forest
3	Green broadleaf forest
4	Senescent broadleaf forest
5	Green woody savanna
6	Senescent woody savanna
7	Green grass savanna
8	Senescent grass savanna
9	Green sparse shrubs
10	Senescent sparse shrubs
11	Water
12	Organic bare soil
13	Arid bare soil
14	Snow, ice

Table 1. Fourteen emissivity classes used in this report, from Snyder et al. *(1998).*

Snyder *et al.*'s analysis used a range of different structural parameters as possible inputs to the BRDF models, and thereby produced a range of emissivity spectra for each class. The spectra were then presented in the Snyder *et al.* paper as a mean value, with an envelope of extreme values lying either side of the mean. The digital data for these 14 class spectra have been obtained from Snyder in this format. Snyder *et al.*'s paper also included some discussion on the viewing-angle dependence of the emissivity, but separate information on this was not included in the data received from Snyder. However, Snyder *et al*. show that the angular effects are small when compared with other uncertainties, at least for most of the emissivity classes considered, and these angular effects have therefore been ignored for the results presented in this report. It may be necessary to revisit this particular aspect at some point in the future.

Two examples of the class spectra are shown in Figure 1, with 1(a) showing the result for green needle forest, and 1(b) for organic bare soil. As in the Snyder *et al*. paper, the solid line represents the mean emissivity, with the dashed line showing the envelope of the extremes. The data are given at 4 cm^{-1} spectral resolution between 750 cm^{-1} and 2750 cm^{-1}. Note that when this atlas is used for spectral intervals outside this range, some thought will have to be given about extrapolating the data in a physically realistic way.

3. LAND COVER CLASSIFICATION DATA

The land cover classification data used for this report are based primarily on the IGBP (International Geosphere Biosphere Programme) classes (Belward 1996), and we have used the global AVHRR-based dataset available via the USGS (United States Geological Survey) EROS Data Center site (details at

http://edcdaac.usgs.gov/glcc/globdoc2_0.html). The spatial resolution of this dataset was originally 0.0083° (i.e. around 1 km), but we have reduced this by a factor 3 to 0.025° for this work. Also, we have extended the number of land cover classes from 17 to 24. The main reason for this increase was to accommodate the additional classes required by Snyder *et al*. (1998), which results in the splitting of some of the IGBP classes into sub-classes. For example, Snyder *et al*.'s technique requires the land cover class "growing broadleaf crops" to be assigned the spectrum corresponding to the emissivity class "green woody savanna", and the land cover class "growing grass crops" to the "green grass savanna" emissivity class. However, the IGBP classification only has "croplands" as a class, and contains no information on whether they are broadleaf or grass crops. Thus we have used data for the Running et al. (1995) classification to split the "croplands" class (no. 12) into "broadleaf crops" (class no. 19) and "grass crops" (class no. 20). In a similar manner, we have used the USGS Land Use/Land Cover System classification data (Anderson et al. 1976) to split the IGBP "vegetation mosaic" class (no. 14) into two sub-classes, those of "cropland/grassland mosaic" (class no. 21) and "cropland/woodland mosaic" (class no. 22), as required for input to the Snyder et al. scheme. Finally, a new "barren tundra" class (no. 18) was created as a sub-class of the IGBP "barren" class (no. 16), in common with relevant studies by Wilber et al. (1999) and Uspensky et al. (2000), and the IGBP "water" class (no. 17) was split into "inland water" (no. 23) and "sea water" (no. 24) classes, though none of these changes was utilised in the current analysis. The extended IGBP classification is shown in Table 2, and the data are plotted in Figure 2.

4. MAPPING THE EMISSIVITY CLASSES ONTO THE LAND COVER CLASSIFICATION DATA

The 14 emissivity classes of Snyder et al. (1998) are mapped onto the extended land cover classes by way of the assignments summarised in Table 3, which closely follows Snyder *et al.*'s Table 2. Note that the "urban" IGBP class has no emissivity class assignment, as this type of surface was not considered in Snyder *et al*.'s study.

What now needs to be considered is how to determine whether a particular pixel should be represented as "green" or "senescent", since this will clearly have a large impact on the emissivity class to which that pixel is assigned. Snyder *et al*. (1998) do not go into detail but suggest that the green/senescent split can be established from the time of year and the vegetation index. The results of Van de Griend and Owe (1993) also suggest a strong correlation between NDVI and surface emissivity. In order to establish some sort of vegetation index climatology, we have made use of 4 years of Pathfinder AVHRR NDVI (Normalised Difference Vegetation Index) data (January 1995 to December 1998), which are available as monthly means from the Goddard Space Flight Center's Distributed Active Archive Center (DAAC) ftp site at ftp://daac.gsfc.nasa.gov/data/avhrr/global_1dg. Note that Pathfinder's NDVI dataset is of highly questionable quality beyond 1998.

As well as constructing average monthly NDVI datasets from the 1995 to 1998 data, we have also constructed maximum and minimum NDVI datasets from the same source data, which we also use in the subsequent analysis. Examples of these data are shown in Figure 3.

Class number	Class name
1	Evergreen needle forest
2	Evergreen broadleaf forest
3	Deciduous needle forest
4	Deciduous broadleaf forest
5	Mixed trees, shrubs
6	Dense shrublands
7	Sparse shrublands
8	Woody savanna
9	Savanna
10	Grasslands
11	Wetlands
12	Croplands
13	Urban
14	Vegetation mosaic
15	Snow, ice
16	Barren
17	Water
18	Barren tundra
19	Broadleaf croplands
20	Grass croplands
21	Cropland/grassland mosaic
22	Cropland/woodland mosaic
23	Inland water
24	Sea water

Table 2: Land cover classes used in this report. The first 17 are taken from the IGBP classification, while numbers 18 to 24 are taken from additional classifications described in the text.

Two different methodologies have been employed in using the NDVI data to determine the green/senescent split for the relevant land cover pixels.

(i) Assume a linear variation for -0.1 < NDVI < 0.85, such that vegetative state is totally senescent for NDVI < -0.1, totally green for NDVI > 0.85, and varies linearly with NDVI for intermediate values. 0.85 and -0.1 represent the highest and lowest values of NDVI typically found in the Pathfinder data used for this work. This will subsequently be referred to as "Method 1".

(ii) Uses pixel-by-pixel annual maximum and minimum NDVI values, and calculates green/senescent split according to the size of the monthly NDVI compared with these maximum and minimum values, again assuming a linear variation with NDVI. This will subsequently be referred to as "Method 2".

For comparison purposes we have also used an additional method whereby the vegetative state is assumed to be totally green at all times, with no variation throughout the year. This will be referred to as "Method 3".

Global plots of the land surface emissivity values, generated for the proposed atlas using methods 1 and 2, are shown in Figures 4 and 5 respectively, for the months of January, April, July and October. These particular emissivity values have been integrated over the filter response function of MODIS band 31 (see Section 5 below), which corresponds to a central wavelength of 11.0 μm.

Both methods seem to show broadly similar patterns of land surface emissivity throughout the annual cycle, with the large increases in vegetation over North America, Europe and northern Asia during the northern hemisphere summer (as seen in the NDVI values in Figure 3) being reflected in significant increases in the 11 μm emissivity for the same areas. However, there are a number of regions where the emissivities predicted by the two methods are significantly different. One example of this is over north west Europe in January, where Method 1 predicts that most of Spain, France and the British Isles have an emissivity around 0.985 (i.e. a red colour in Figure 4), whereas Method 2 suggests these areas generally having lower emissivities around 0.975 (i.e. a green colour in Figure 5). Other areas having significant discrepancies between the two methods include: South America in July and October; Kazakhstan (north of the Caspian and Aral Seas) in April, July and October; south east Australia in January and April; and central and southern Africa during all four months.

Snyder et al. (1998) emissivity class	Extended IGBP class
Green needle forest	Evergreen needle forest, Green deciduous needle forest
Senescent needle forest	Senescent deciduous needle forest
Green broadleaf forest	Evergreen broadleaf forest, Green deciduous broadleaf forest, Green mixed trees and shrubs
Senescent broadleaf forest	Senescent deciduous broadleaf forest, Senescent mixed trees and shrubs
Green woody savanna	Green woody savanna, Green crop/tree mosaic, Growing broadleaf crops
Senescent woody savanna	Senescent woody savanna, Senescent crop/tree mosaic
Green grass savanna	Green savanna, Green grasslands, Green dense shrublands, Growing grass crops, Green crop/grass mosaic
Senescent grass savanna	Senescent savanna, Senescent grasslands, Senescent dense shrublands, Senescent crop/grass mosaic
Green sparse shrubs	Green sparse shrublands
Senescent sparse shrubs	Senescent sparse shrublands
Water	Inland water, Wetlands
Organic bare soil	Idle broadleaf crops, Idle grass crops
Arid bare soil	Barren
Snow, ice	Snow, ice

Table 3. Correspondence between the fourteen Snyder et al. emissivity classes and the extended IGBP land cover classes associated with each one (adapted from Snyder et al. 1998).

5. MODIS DATA PRODUCTS USED FOR COMPARISONS

The MODIS (Moderate Resolution Imaging Spectroradiometer) instrument on board NASA's Terra satellite routinely retrieves Land Surface Temperature (LST) products, and included in those products are associated land surface emissivity (LSE) data. Provisional data have been available for these products since 1st November 2000, and can be accessed free of charge via the following URL: http://edcimswww.cr.usgs.gov/pub/imswelcome/.

Two methods have been used in the derivation of MODIS LST products. The first uses a "split-window" approach, utilising MODIS bands 31 (centred at 11.0 μm) and 32 (12.0 μm), and applies emissivity class data to land cover class data in a similar manner to that used for the current LSE atlas development work described above. Therefore, it is the LSE data from this product which have been used for our initial comparisons. These data are available at 1 km spatial resolution. In terms of temporal resolution, the data are available as individual swath data (product code MOD11_L2), 1-day averages (MOD11A1) and 8-day averages (MOD11A2).

A second MODIS LST/E product (MOD11B1) is available which uses an algorithm applied to pairs of MODIS day-time and night-time observations. This method retrieves simultaneously the land-surface temperature and emissivities in bands 20 (centred at 3.75 μm), 22 (3.96 μm), 23 (4.05 μm) and 29 (8.55 μm), as well as the bands (31 and 32) used for the first method. The data are available at 5 km spatial resolution, and are daily averages. We shall mainly be carrying out comparisons with these data in a future report, although some discussion of them is included in Section 9 below.

6. REGIONAL COMPARISONS BETWEEN THE GENERATED EMISSIVITIES AND MODIS PRODUCTS

Initially, we will show comparisons for a small number of selected geographic regions where discrepancies have been noted between the two methods discussed in Section 4 of this report. These comparisons will be made using products for MODIS band 31, centred at 11.0 μm. The emissivities predicted by the various methods outlined in Section 4 above have therefore been integrated over the filter response function of this channel.

Figure 6 shows daily composites of the MOD11_L2 swath data for band 31 (labelled as "Retrieved MODIS 31 surface emissivity" in subsequent plots) from south east Australia for 16/1/2001, 16/4/2001, 16/7/2001 and 16/10/2001. The land areas which are white have no surface emissivity values present for that day due to the presence of cloud during all relevant overpasses.

This figure shows that the emissivities basically fall into two categories here, and comparison with the land cover dataset indicates that these values are associated with the "sparse shrublands" land cover class, with emissivities of around 0.972, and those associated with more densely vegetated classes (evergreen broadleaf forest, woody savanna, savanna, broadleaf cropland and grass cropland), with emissivities of around 0.986. This latter value corresponds much more closely with the "green" rather than the "senescent" state of these classes when compared with the Snyder *et al*. emissivity class data. The MOD11_L2 emissivity values show very little variation between the four seasons, which is perhaps

a little surprising, given that the maximum and minimum NDVI data for this region (Figures 3c and 3d) do indicate that the vegetative state varies significantly throughout the annual cycle.

Figure 7 shows a comparison for this region between the MOD11_L2 band 31 emissivity product for 16/4/2001 and the emissivities calculated for April using Methods 1 and 2 described in Section 4 above, together with the emissivity from Method 3, which does not vary with season. The agreement is reasonable in all three cases. In terms of the spatial pattern of the emissivities, Method 3 seems to produce the closest agreement with the MOD11_L2 data. Methods 2 and 3 also produce reasonable agreement for the most part, but some regions of intermediate emissivity (0.975-0.980) exist which are not present in the MOD11_L2 data. A similar comparison for July is shown in Figure 8. In this case, all three methods are seen to give very good agreement with the MOD11_L2 product.

Figure 9 shows daily composites of the MOD11_L2 swath data for band 31 from central South America for 16/1/2001, 16/4/2001, 16/7/2001 and 16/10/2001. In this case the emissivities fall into three broad categories. These represent the "sparse shrublands" class (with emissivities of around 0.972) and the more densely vegetated classes (with emissivities of around 0.986), as for the south eastern Australia case shown in Figure 6, together with a region corresponding to the "barren" IGBP land cover class, which has a lower emissivity value of around 0.966. Again, the 0.986 emissivity value for the densely vegetated classes corresponds much more closely with the "green" rather than the "senescent" state of these classes when compared with the Snyder *et al*. data. Once again, the MOD11_L2 emissivity values show little or no variation between the four seasons.

Figure 10 shows a comparison for the same region between the MOD11_L2 band 31 emissivity product for 16/1/2001, and the emissivity calculated for January using Methods 1, 2 and 3 described above. Again, the agreement is reasonable in all three cases. This time, the Method 3 approach underestimates the amount of land corresponding to the intermediate (0.975-0.980) emissivity values, and it is Method 1 which produces the best agreement with the MOD11_L2 product. Method 2 is also seen to produce reasonable agreement, with the exception of some areas around Uruguay, which have predicted emissivities of around 0.978, lower than the corresponding MOD11_L2 values.

Figure 11 shows a similar comparison for October, and basically tells the same story, with Method 3 and, in particular, Method 1 showing very good agreement with the data. For method 2, the agreement is worse than it was for the January comparison, and there are significant areas where emissivities of around 0.978 predicted by this method are lower than the values of around 0.985 in the MOD11_L2 data.

Turning to the central African region, Figure 12 shows daily composites of the MOD11_L2 band 31 swath data for 16/1/2001, 16/4/2001, 16/7/2001 and 16/10/2001. As before, the emissivities fall into three broad categories. These represent the Saharan region to the north of the images, where a "barren" IGBP land cover class yields an emissivity of around 0.966 for band 31, a very narrow "sparse shrublands" class with emissivities of around 0.972, and the more densely vegetated tropical region to the south of the images, with emissivities of around 0.986 (once again corresponding closely to the "green" state of these classes when compared with the Snyder *et al*. data).

Figure 13 shows a comparison for this region between the MOD11_L2 band 31 emissivity data for 16/1/2001, and the emissivities calculated for January using Methods 1, 2 and 3. Here, the agreement is significantly better with Method 3 than with either Methods 1 or 2. These two methods predict the occurrence of a wide belt of land having emissivities of around 0.97-0.98 being situated between the Saharan region to the north and the densely vegetated tropical region to the south. The MOD11_L2 data do not show this, however, and agree very well with the Method 3 image. Figure 14 shows a similar comparison for October, and, although the Methods 1 and 2 predictions do give somewhat better agreement with the MOD11_L2 data, Method 3 again provides the closest match.

Figure 15 shows 8-day averages of the MOD11A2 band 31 data from western Europe and northern Africa for the periods 9/1/2001-16/1/2001, 15/4/2001-22/4/2001, 12/7/2001-19/7/2001 and 16/10/2001-23/10/2001. We have used the MOD11A2 data here rather than the MOD11_L2 swath data used previously, because high incidences of cloud in the swath data on the individual days precluded making any meaningful comparisons with them. Note that the MOD11A2 product is only available on an integerised sinusoidal projection, so the MOD11A2 images presented in Figures 15 to 18 are on a different projection from the standard geographic projection used elsewhere in this report. It can be seen that large parts of the area have emissivities of around 0.985, corresponding to green vegetation of one sort or another. Some lower emissivity values exist in central Spain, and also in the transition region just north of the Sahara Desert, where the emissivities decrease to values of around 0.960.

Figure 16 shows a comparison for this region between the MOD11A2 band 31 emissivity data for 9/1/2001-16/1/2001, and the emissivities calculated for January using Methods 1, 2 and 3. Again, the agreement is significantly better with Method 3 than with either Methods 1 or 2. Method 3 generally reproduces the MOD11A2 emissivities well, with the exception of some areas of lower emissivity over Spain, and a slight discrepancy in the emissivity value over the Sahara. Method 1 predicts that a significant area to the eastern side of the image has emissivities lower than in the retrieved MODIS data, and Method 2 performs even worse in this regard.

Figures 17 and 18 show comparisons over the same area for July and October respectively. For these two cases, Method 3 is again reasonable, as noted above, but Methods 1 and 2 are generally in much better agreement with the MOD11A2 products than for the January case. Method 1 is in particularly good agreement with the retrieved MODIS data for these two months, producing very similar-looking distributions of emissivity over areas such as Spain, northern Africa and the Alps.

Note that Snyder *et al*.'s emissivity classes (Table 1) make no provision for the "urban" land class. For the atlas plots shown in this section of the report, the surface emissivity was set to 0.965 (based on a very preliminary look at some of the MOD11A2 data shown in Figures 16 to 18) for any land pixels classed as being "urban" in the IGBP dataset. This subject will be looked at in more detail in Section 8 below.

Figure 19 shows daily composites of the MOD11_L2 band 31 swath data for 16/1/2001, 16/4/2001, 16/7/2001 and 16/10/2001, for an area of Asia centred on Kazakhstan in the vicinity of the Caspian and Aral Seas. Some of these images, in particular the ones for April and (to a lesser extent) October,

appear somewhat noisy, with rather artificial-looking lines of high (around 0.992) emissivity being interspersed with regions of lower emissivity. Also relevant to this discussion is that fact that, for the winter months at least, a large part of this region will have been snow-covered.

In order to assess which areas were affected by snow during these periods, we have looked at some images from the NESDIS Operational Daily Snow Cover Analysis product, available via the link http://www.ssd.noaa.gov/PS/SNOW/index.html. Images for Europe/Asia for 16/1/2001, 16/4/2001, 16/7/2001 and 16/10/2001 are shown in Figure 20.

These images show that for 16/1/2001 the southern edge of the snow cover is situated roughly halfway down the eastern shore of the Caspian Sea, and lies entirely to the south of the Aral Sea, implying that most of the upper half of the January image in Figure 19 would be affected. In fact, on closer inspection, it appears that most, if not all, of the areas of high (i.e. around 0.992) emissivity present in the January image in Figure 19 (given by the orange colour) correspond to snow-covered areas on the relevant image in Figure 20. It should be noted that the inverse is not always true, in that not all of the snow-covered areas in Figure 20 correspond to high emissivity areas in Figure 19.

For 16/4/2001, the snow edge has moved further north in the NESDIS analysis. For the most part, the "noisy" high emissivity (orange) lines are also further north in the MOD11_L2 data. For the July and October images in Figure 20, the snow lies well to the north of the area in question. It seems possible therefore that these orange areas of higher emissivity in the MOD11_L2 products are associated with the presence of snow on the ground, although why they should appear in such a noisy fashion is not clear at present.

It makes sense, therefore, to restrict comparisons in this case to areas which are likely to be clear of snow, i.e. the more southern parts of the region for the January and April images, and the whole region for the July and October images. Having done so, it is once again noted that, in common with the other comparison regions used above, the MOD11_L2 product shows no significant variation throughout the annual cycle.

Figure 21 shows a comparison for this region between the MOD11_L2 band 31 emissivity data for 16/1/2001, and the emissivities calculated for January using Methods 1, 2 and 3. Even allowing for the fact that we are restricting our comparison to the snow-free areas (i.e. only the lower portion of the images), the agreement between Methods 1 and 2 and the MOD11_L2 data is not particularly good. In barren areas, the emissivities are similar (i.e. around 0.965), whereas for the vegetated areas, Methods 1 and 2 predict values around 0.97-0.98 (green colours in Figure 21), whereas the MOD11_L2 data show emissivities up to 0.986 (red colours). The agreement between Method 3 and the MOD11_L2 data is significantly better for the snow-free areas of Figure 21.

Figure 22 shows a comparison for the same region between the MOD11_L2 band 31 emissivity data for 16/4/2001, and the emissivities calculated for April using Methods 1, 2 and 3. The relevant snow cover analysis from Figure 20 suggests that perhaps the uppermost third of the region in Figure 22 is snow-covered, so we restrict our comparisons to the lower two-thirds of the image.

The agreement between the Method 1 emissivities and the MOD11_L2 data is somewhat better than for the January case, although there is still a tendency for the emissivity to be too low for Method 1. Most significantly, a large area of land lying just to the north of the Caspian and Aral Seas, which is associated with grassland in the IGBP dataset, has an emissivity of around 0.975 for the Method 1 simulation, but a value of around 0.985 in the MOD11_L2 data. The agreement is much better for the case of Method 2, including this grassland area. Method 3 is also seen to be in good agreement with the MOD11_L2 data for the snow-free areas.

Figure 23 shows one further comparison for the Kazakhstan region between the MOD11_L2 band 31 emissivity data for 16/7/2001, and the emissivities calculated for July using Methods 1, 2 and 3. The relevant snow cover analysis from Figure 20 suggests that this region was entirely free from snow at this time of year. The agreement between Method 1 and the MOD11_L2 data is reasonably good, although again there is a significant discrepancy in the grassland area to the north of the Caspian and Aral Seas, where the Method 1 emissivity of around 0.975 is lower than the MOD11_L2 emissivity of around 0.985 in band 31. Methods 2 and 3 are in much better agreement with the MODIS product, as was the case for April.

7. GLOBAL COMPARISONS BETWEEN THE GENERATED EMISSIVITIES AND MODIS PRODUCTS

Having looked at some regional comparisons, where we focussed on regions where the different methods outlined in Section 4 produced differing emissivity values, we now turn to some global comparisons. Because of the large quantity of MOD11_L2 data granules involved in making a global composite, we have restricted the comparisons to just two time periods, those of 16 - 17/1/2001 and 16 - 17/7/2001. These comparisons will be made using products for MODIS band 31, centred at 11.0 μm, as in Section 6 above, and also for MODIS band 32, centred at 12.0 μm. A two-day period was chosen in order to increase the likelihood of obtaining cloud-free pixels for a greater proportion of the Earth's surface.

Figure 24 shows a global comparison between the MOD11_L2 band 31 (11.0 μm) emissivity for 16-17/1/2001 and the emissivities calculated for January using Methods 1, 2 and 3. The agreement is seen to be reasonable for both Methods 1 and 2, but in common with the regional comparisons presented above, significant discrepancies do exist. For example, large parts of North America, Europe and Asia are assigned emissivities of around 0.975 (green) in both the Method 1 and 2 schemes, whereas the MOD11_L2 data generally indicate emissivities of around 0.985 (red). In addition, the retrieved MODIS data for these regions also contain sizeable areas of even higher emissivity (around 0.992, orange), which, as discussed previously, may be associated with snow cover. In fact, as seen in Figure 20, a large part of northern Asia is indeed covered by snow at this time of year (as is the case for North America). Other areas where significant discrepancies exist include central Africa, south west Africa, south east Asia and Australia. In all of these regions, to a greater or lesser extent, one or both of Methods 1 and 2 predict emissivities which are lower than indicated by the MOD11_L2 data. The agreement between Method 3 and the MODIS product is significantly better, certainly in terms of its spatial pattern, although the absolute values of the emissivities are still somewhat different.

One final discrepancy which is worth pointing out is over areas classified as being snow or ice by the IGBP dataset (i.e. Greenland and Antarctica). The Snyder emissivity class of "snow, ice", when integrated over the response function of MODIS band 31, yields an emissivity value of 0.988, which is what is given by all three methods used above. The MOD11_L2 data give a somewhat higher value of around 0.993 for these regions.

The equivalent global comparison for July is shown in Figure 25, where the MOD11_L2 data are from 16-17/7/2001. Note that the January and July MOD11_L2 images are very similar to one another in the areas likely to have been free of snow. The agreement between the retrieved MODIS data and both Methods 1 and 2 is much better than for the January comparison shown in Figure 24, possibly because of the absence of snow over the majority of North America, Europe and northern Asia. However, there are still several regions where significant discrepancies exist, including central and southern Africa, central and southern Asia and the southern part of South America, where again, to a greater or lesser extent, one or both of Methods 1 and 2 predict emissivities which are lower than indicated by the MOD11_L2 data. The agreement between Method 3 and the MODIS product is again significantly better in general. As for the January comparison shown in Figure 24, the discrepancies in areas classified as being snow or ice remain.

Figure 26 is similar to Figure 24, only this time uses MOD11_L2 band 32 (12.0 μm) emissivity for 16-17/1/2001, rather than band 31 (11.0 μm). As was the case with band 31, large parts of North America, Europe and Asia are assigned relatively low emissivities (of around 0.975, green) in both the Method 1 and 2 schemes when compared with the MOD11_L2 values of around 0.990 (orange). Other areas where notable discrepancies exist include central Africa, south east Asia and Australia, particularly for Method 2. The agreement between Method 3 and the MODIS product is significantly better than for the first two methods once again.

However, as was the case for the band 31 (11.0 μm) comparison, there is a significant discrepancy in surfaces classified as snow or ice by the IGBP dataset. The Snyder emissivity class of "Snow, ice", when integrated over the response function of MODIS band 32, yields an emissivity value of 0.978, which is what is given by all three methods used above. The MOD11_L2 data give a significantly higher value of around 0.989 for these regions.

The equivalent global comparison for July is shown in Figure 27, where the MOD11_L2 band 32 (12.0 μm) data are from 16-17/7/2001. The agreement between the retrieved MODIS data and the emissivities predicted by all three methods is reasonable in this instance, although, as for the January comparison shown in Figure 25, the discrepancies in regions classified as being snow- or ice-covered are significant.

8. TUNING THE SCHEMES TO GIVE OPTIMUM AGREEMENT WITH THE MODIS SPLIT-WINDOW LAND SURFACE EMISSIVITY PRODUCT

The comparisons presented in Sections 6 and 7 above indicate, perhaps contrary to expectations, that the MODIS split-window emissivity products (i.e. MOD11_L2 and MOD11A2) show little or no

variation throughout the annual cycle. Thus, we have seen that the first two methodologies used to develop time-varying surface emissivity maps by using monthly-averaged NVDI values often produce poor agreement when compared with the MODIS split-window emissivities. Method 3, which has no time-dependence (i.e. does not depend upon the NDVI values), and for which we have assumed a vegetative state of 100% "green" at all times, seems to show much better agreement with the MOD11_L2 values in general. However, there are still several instances where we have shown that, although the general spatial patterns of emissivity are quite well represented by Method 3, there are still some areas and land types where the absolute values of emissivity predicted by Method 3 are somewhat different from the MOD11_L2 data. Thus, it might be possible to "tune" the green/senescent split to a value other than 100% green to yield better agreement with the MODIS split-window emissivities.

As well as the MODIS land surface temperature/emissivity product (MOD11), MODIS products also exist for Land Cover (MOD12) and Vegetation Index (MOD13). Because the main land type classification used for MOD12 is based on the IGBP classification, then as well as simply comparing maps of surface emissivity, it is also possible to examine quantitatively the surface emissivity product as a function of land type and NDVI, in order to confirm our earlier finding that the MODIS split-window emissivities do not show any dependence on the annual (and hence vegetative) cycle, and also establish the required green/senescent ratio required to give best agreement with the MODIS emissivities for each land type.

To do this, therefore, we have extracted data for each of these three products for three geographic locations (in North America, South America and central Russia) over the course of one year (2001). Analysis of these data confirms that the surface emissivity for a particular land type does not vary in any systematic way with the corresponding value of NDVI. It also shows that, in general, the choice of 100% green for the senescent state (where appropriate) is indeed not the optimum choice if obtaining agreement with the MODIS split-window emissivities is the aim, and that some other fractional split, which varies from one surface type to another, tends to produce better agreement. The green/senescent ratios which do provide the best agreement on average for each surface type are shown in Table 4 below.

Another significant difference, which was noted in Section 7 above, is that there are substantial discrepancies at both 11.0 μm and 12.0 μm when the Snyder-based emissivities for the "Snow/ice" land-covered areas are compared with the corresponding MOD11_L2 values. The Snyder *et al.* (1998) data, when averaged over the spectral response functions of MODIS bands 31 and 32, give emissivities of 0.988 and 0.978 respectively, whereas the MOD11_L2 data suggest average values around 0.993 and 0.989 respectively.

In order to provide a means of tuning the emissivity atlas to give better agreement with the MODIS split-window emissivity product, a number of other relevant emissivity spectra were obtained from different sources, including the Salisbury *et al.* (1994) and Snyder *et al.* (1997) datasets (digital data for both these datasets were kindly supplied by Dr. Will Snyder), the JPL ASTER spectral library (accessible via the URL http://speclib.jpl.nasa.gov/) and the ICESS/UCSB (Institute for Computational Earth System Science, University of California, Santa Barbara) emissivity library (via the URL

http://www.icess.ucsb.edu/modis/EMIS/html/em.html). These data were analysed to find whether any of the spectra, or some combination of them, could provide better agreement with the MODIS split-window emissivity data at 11.0 μm and 12.0 μm.

In general, the data proved to be somewhat difficult to fit at 12.0 μm, with most of the spectra giving emissivities significantly below the mean MODIS band 32 value of 0.989. However, it was found that a linear combination of 60% "fresh frost" and 40% "medium granular & disaggregated granular snow" (both spectra taken from the Salisbury *et al.* 1994 dataset) were able to produce a reasonable match at the two wavelengths, yielding emissivities of 0.993 and 0.988 for MODIS bands 31 and 32 respectively. It should be stressed that this solution is somewhat *ad hoc* and has not been compared with data at other wavelengths, and so should be treated with caution at this stage.

Finally, we address the issue of what emissivities to use for pixels corresponding to a land class of "urban". Analyses of MOD11A2 emissivity data, such as those shown in Figures 15 to 18, together with the relevant MODIS land classification data also mentioned above, indicate that the mean values of surface emissivity for bands 31 and 32 are around 0.976 and 0.980 respectively, although there is considerable variability around these values. As was done for the "snow/ice" class considered above, a number of other relevant emissivity spectra were obtained from the different datasets available, and these were analysed to find a suitable combination which provided agreement with the MODIS split-window emissivities at 11.0 μm and 12.0 μm.

It was found that a linear combination of 20% "natural masonry", 10% "red masonry", 18% "tan masonry", 46% "mixed trees, shrubs" and 6% "barren" produced good agreement at the two wavelengths, yielding the required emissivities of 0.976 and 0.980 for MODIS bands 31 and 32 respectively. The three "masonry" emissivity spectra were all taken from the ICESS dataset referred to above, and the "mixed trees, shrubs" and "barren" spectra were constructed from Snyder *et al*. (1998) spectra as indicated in Table 4. Again, it should be stressed that this solution is somewhat *ad hoc*, in that it has only been constrained by information at two wavelengths, and should therefore be treated with caution at this stage.

Comparisons between MOD11_L2 values for January and July 2001 and the "tuned" emissivities described above (labelled as Method 4) are shown in Figures 28 and 29. It will be seen that the agreement has improved significantly, as expected, especially for the "snow/ice" regions (i.e. Greenland and Antarctica).

9. Discussion & Conclusions

We have developed a scheme for producing global maps of land surface emissivity at thermal infrared wavelengths, by coupling a land cover classification dataset with different classes of surface emissivity spectra. We have compared the derived emissivities with values taken from the MODIS land surface temperature/emissivity split-window products (MOD11_L2 and MOD11A2). By using a suitable "tuning" of the split between the green and senescent contributions for vegetated land pixels, we were

able to obtain good agreement, although further analysis using additional emissivity spectra was required for the land pixels classified as "snow/ice".

Class number	Class name	Emissivity spectra used
1	Evergreen needle forest	100% green needle forest
2	Evergreen broadleaf forest	100% green broadleaf forest
3	Deciduous needle forest	100% senescent needle forest
4	Deciduous broadleaf forest	94% green broadleaf forest, 6% senescent broadleaf forest
5	Mixed trees, shrubs	90% green broadleaf forest, 10% senescent broadleaf forest
6	Dense shrublands	51% green grass savanna, 49% senescent grass savanna
7	Sparse shrublands	100% green sparse shrubs
8	Woody savanna	84% green woody savanna, 16% senescent woody savanna
9	Savanna	91% green grass savanna, 9% senescent grass savanna
10	Grasslands	91% green grass savanna, 9% senescent grass savanna
11	Wetlands	100% water
12	Croplands	85% green woody savanna, 15% organic bare soil
13	Urban	20% natural masonry (ICESS), 10% red masonry (ICESS), 18% tan masonry (ICESS), 46% "mixed trees, shrubs" (see class 5), 6% "barren" (see class 16)
14	Vegetation mosaic	87% green woody savanna, 13% senescent woody savanna
15	Snow, ice	60% fresh frost (Salisbury), 40% medium granular & desegregated granular snow (Salisbury)
16	Barren	100% arid bare soil
17	Water	100% water
18	Barren tundra	100% arid bare soil
19	Broadleaf croplands	85% green woody savanna, 15% organic bare soil
20	Grass croplands	85% green grass savanna, 15% organic bare soil
21	Cropland/grassland mosaic	87% green grass savanna, 13% senescent grass savanna
22	Cropland/woodland mosaic	87% green woody savanna, 13% senescent woody savanna
23	Inland water	100% water
24	Sea water	100% water

Table 4: Emissivity spectra used to produce the atlas dataset labelled as Method 4, which provides optimum agreement with the land surface emissivity values in the MOD11_L2 product at 11.0 μm and 12.0 μm. Most emissivity spectra are taken from Snyder et al. (1998), although some, where indicated, use alternative sources of data from the Salisbury et al. (1994) and ICESS datasets (see text for full details).

It is anticipated that this tuned dataset (Method 4) will be used initially as the basis for the "first guess" surface emissivity within the OPS 1D-Var stage of the HIRS and/or AIRS radiance assimilation for the Met Office global NWP model. Given this fact, it is certainly worthwhile asking the question at this stage, how accurate are these emissivities likely to be? Just because we have obtained what seems to be very good agreement with the MODIS split-window product emissivities is no guarantee that these values are accurate. As was mentioned in Section 5 above, some daily surface emissivity values are also available, at a lower spatial resolution, from an alternative MODIS product, the so-called day/night

algorithm (MOD11B1). Figure 30 shows examples of global emissivity maps from this product, again for MODIS bands 31 and 32 (11.0 μm and 12.0 μm), for 16/2/2001 and 16/7/2001, for comparison with the split-window product emissivities which can be seen in Figures 28 and 29 (note that, as with the MOD11A2 product, the MOD11B1 product is only available on an integerised sinusoidal projection).

Comparisons between the day/night emissivities in Figure 30 and the split-window emissivities in Figures 28 and 29 immediately show large differences between the two algorithms (note the different colour scale). For much of the globe, the MOD11B1 values are of the order 0.94 - 0.96 for both 11.0 μm and 12.0 μm bands, i.e. significantly lower than the corresponding split-window emissivities. Also, the MOD11B1 emissivities of around 0.90 over Antarctica are much lower than their MOD11_L2 counterparts. Other points of interest include the fact that there are some differences between January and July in the day/night product, e.g. the emissivity seems to be significantly higher over much of southern Africa in July than in January. Also, there seem to be only very small differences between bands 31 and 32 in the MOD11B1 emissivities, which was not the case for the split-window products. It seems clear, the emissivity values available from the MODIS split-window emissivity product have a very strong prior-dependence, whereas the MODIS day/night product uses measured information to a larger extent to derive the retrieved emissivities. Further detailed comparisons are beyond the scope of the current study, and will be shown in future reports. For now, this brief comparison serves only to highlight the uncertainties still associated with the emissivities derived as part of current methodology.

Further comparisons which may help to identify the causes of these discrepancies need to be made with MODIS-Aqua products when they become available. Also, work currently in progress comparing the atlas with ARIES data from several MRF aircraft campaigns will prove important in determining the direction in which this work should progress for future studies.

10. REFERENCES

Anderson, J.R., E.E. Hardy, J.T. Roach and R.E. Witmer, 1976: A land use and land cover classification system for use with remote sensor data. *U.S. Geological Survey Professional Paper 964, 28 pp.*

Belward, A.S., ed., 1996: The IGBP-DIS global 1 km land cover data set (DISCover) - proposal and implementation plans. *IGBP-DIS Working Paper No. 13, Toulouse, France, 61 pp.*

Li, Z. and A.H. Strahler, 1992: Geometric-optical bidirectional reflectance modelling of the discrete crown vegetation canopy: Effect of crown shape and mutual shadowing. *IEEE Transactions on Geoscience and Remote Sensing,* **30,** *276-291.*

Roujean, J., M. Leroy and P. Deschamps, 1992: A bidirectional reflectance model of the earth's surface for correction of remote sensing data. *Journal of Geophysical Research,* **97,** *20455-20468.*

Running, S.W., T.R. Loveland, L.L. Pierce, R.R. Nemani and E.R. Hunt, 1995: A remote sensing based vegetation classification logic for global land cover analysis: *Remote Sensing of Environment ,* **51,** *3948-3952.*

Salisbury, J.W. and D.M. D'Aria, 1992: Emissivity of terrestrial materials in the 8-14 μm atmospheric window. *Remote Sensing of Environment,* **42,** *83-106.*

Salisbury, J.W. and D.M. D'Aria, 1994: Emissivity of terrestrial materials in the 3-5 μm atmospheric window. *Remote Sensing of Environment,* **47,** *345-361.*

Salisbury, J.W., D.M. D'Aria and A. Wald, 1994: Measurements of thermal infrared spectral reflectance of frost, snow, and ice. *Journal of Geophysical Research,* **99,** *24235-24240.*

Snyder, W.C., Z. Wan, Y. Zhang and Y.-Z. Feng, 1997: Thermal infrared (3-14 μm) bidirectional reflectance measurements of sands and soils. *Remote Sensing of Environment,* **60,** *101-109.*

Snyder, W.C. and Z. Wan, 1998: BRDF models to predict spectral reflectance and emissivity in the thermal infrared. *IEEE Transactions on Geoscience and Remote Sensing,* **36,** *214-225.*

Snyder, W.C., Z. Wan, Y. Zhang and Y.-Z. Feng, 1998: Classification-based emissivity for land surface temperature measurement from space. *International Journal of Remote Sensing,* **19,** *2753-2774.*

Uspensky, A.B., A.N. Trotsenko, K.A. Il'yachenko and T.A. Udalova, 2000: Derivation of land surface skin temperature and surface emissivity from IASI measurements in clear-sky conditions. *Russian Research Centre "Kurchatov Institute", preprint IAE-6190/16.*

Van de Griend, A.A., and M. Owe, 1993: On the relationship between thermal emissivity and the normalized difference vegetation index for natural surfaces. *International Journal of Remote Sensing,* ***14,*** *1119-1136.*

Wan, Z. and J. Dozier, 1996: A generalized split-window algorithm for retrieving land-surface temperature from space. *IEEE Transactions on Geoscience and Remote Sensing,* **34,** *892-905.*

Wilber, A., D.P. Kratz and S.K. Gupta, 1999: Surface emissivity maps for use in satellite retrievals of Longwave Radiation. *NASA Technical Publication, TP-1999-209362, 35 pp.*

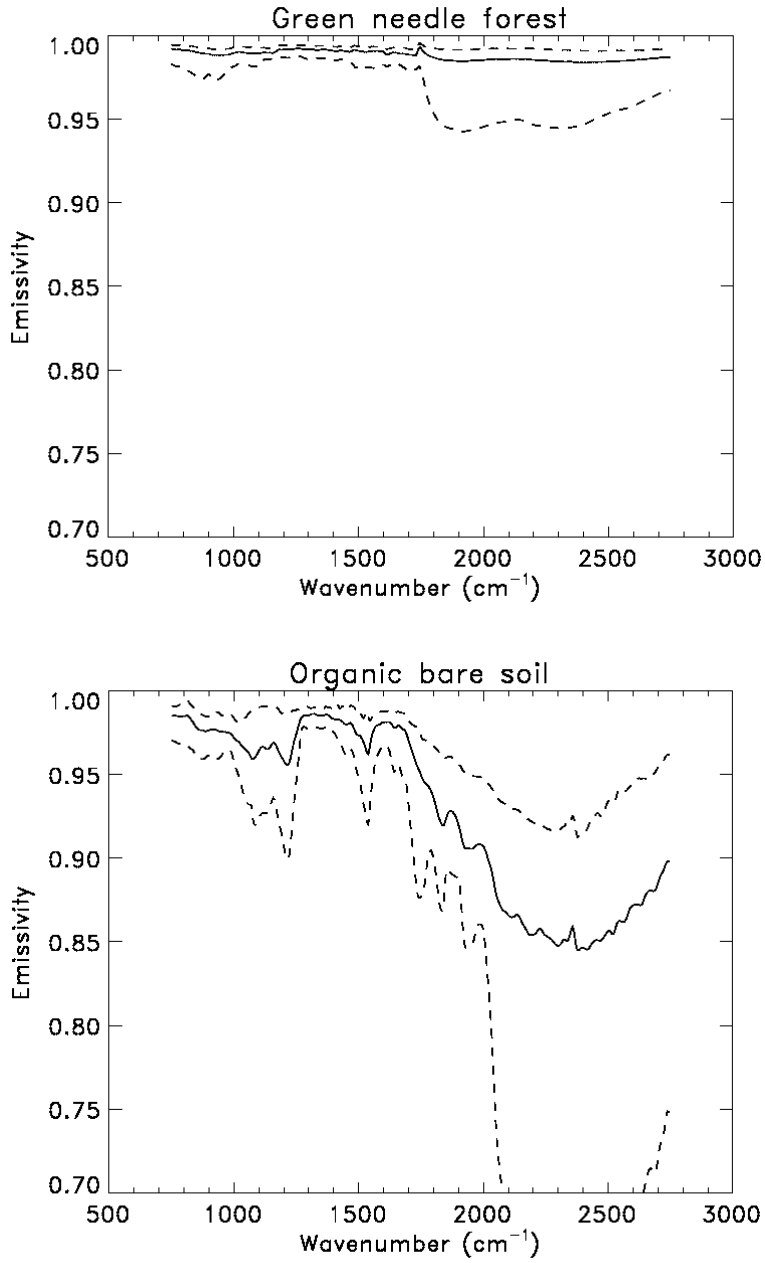

Figure 1: Two examples of emissivity class spectra from Snyder et al. *1998. (a) Green needle forest. (b) Organic bare soil. The solid line corresponds to the average spectrum in each case, with the dashed lines showing the envelope of the extremes.*

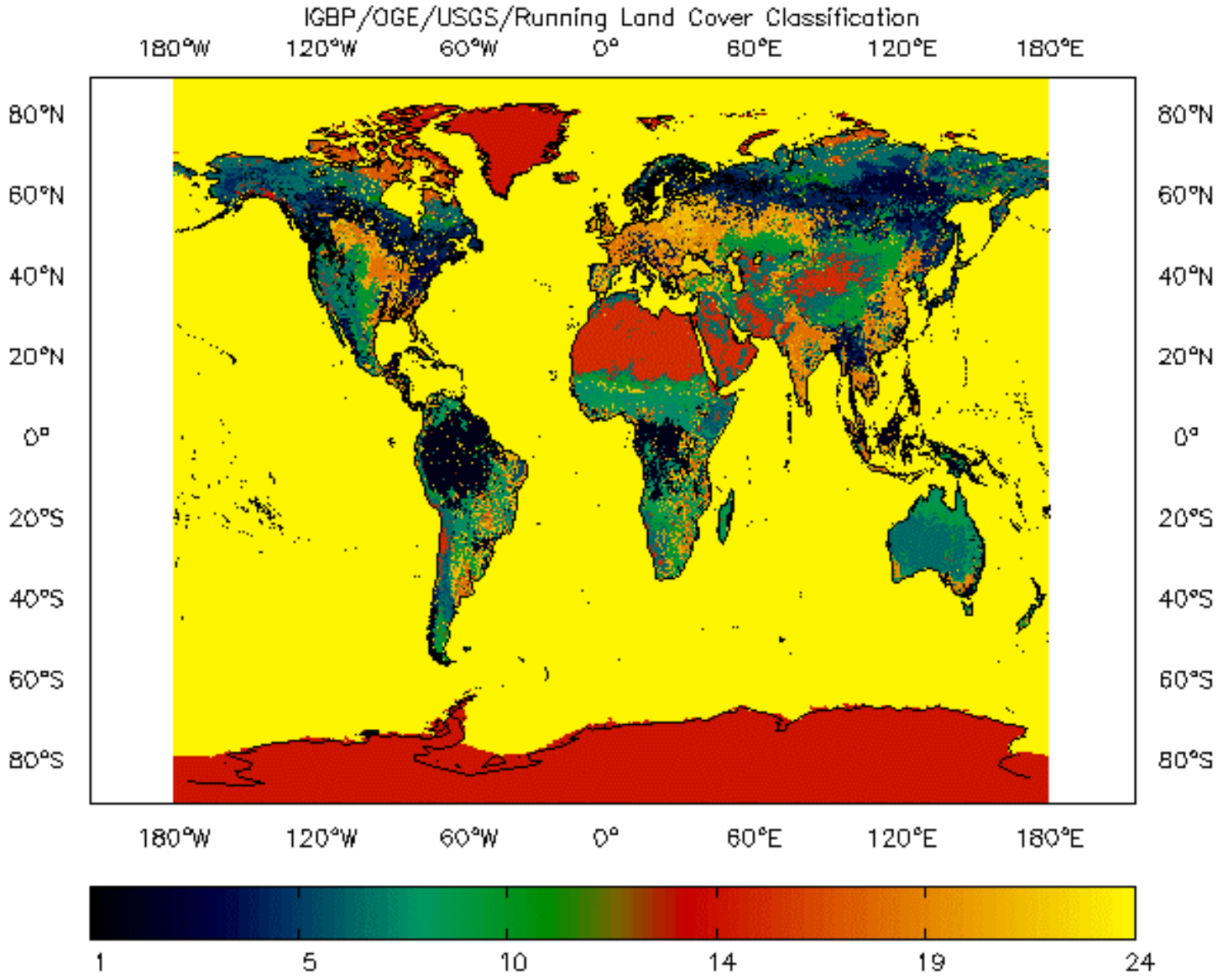

Figure 2. Extended IGBP land cover classes (see text for full details).

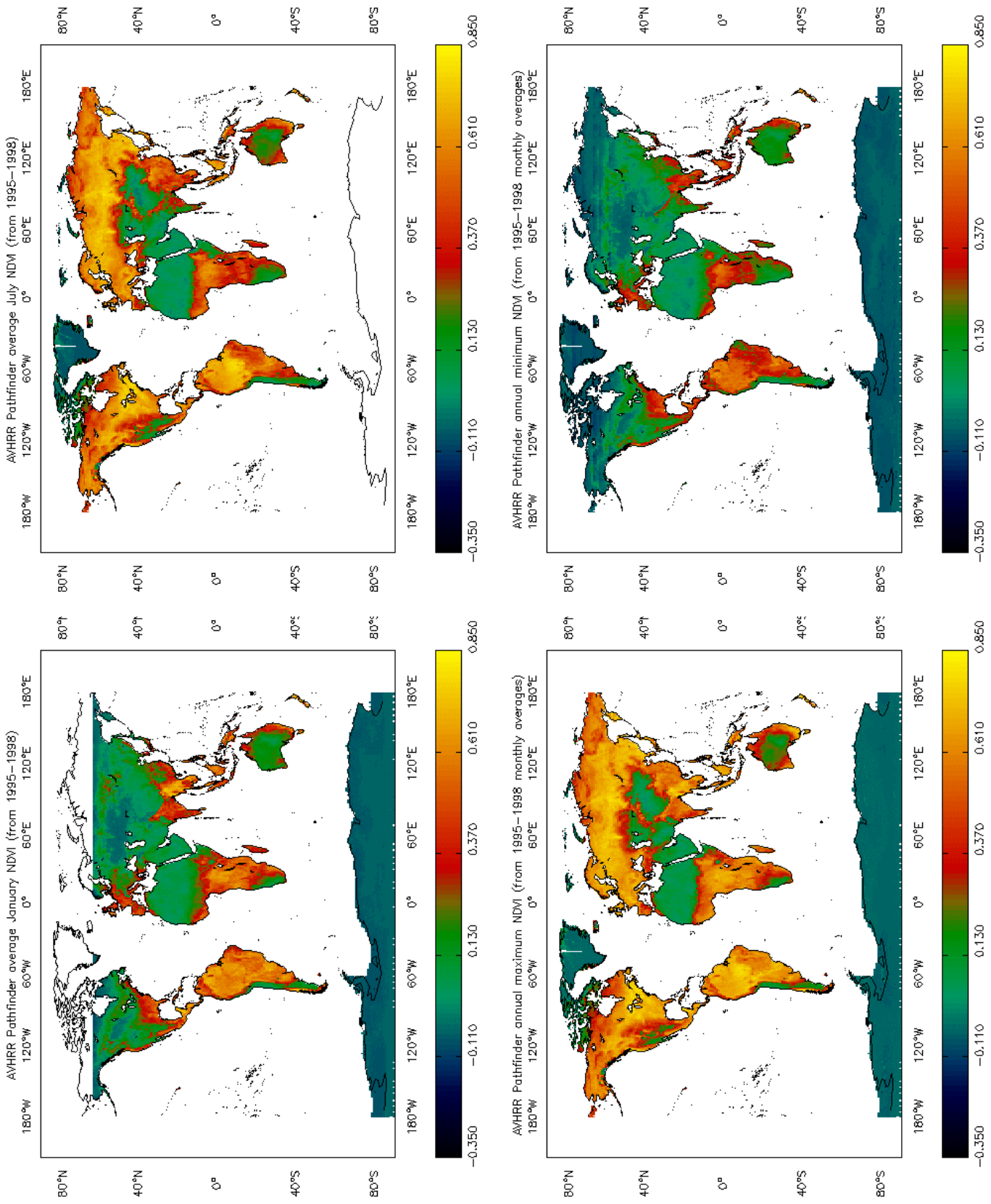

Figure 3: Examples of 1995-1998 Pathfinder AVHRR NDVI data used in the present study. (a) January average. (b) July average. (c) Annual maximum NDVI from 1995-1998 monthly averages. (d) Annual minimum NDVI from 1995-1998 monthly averages.

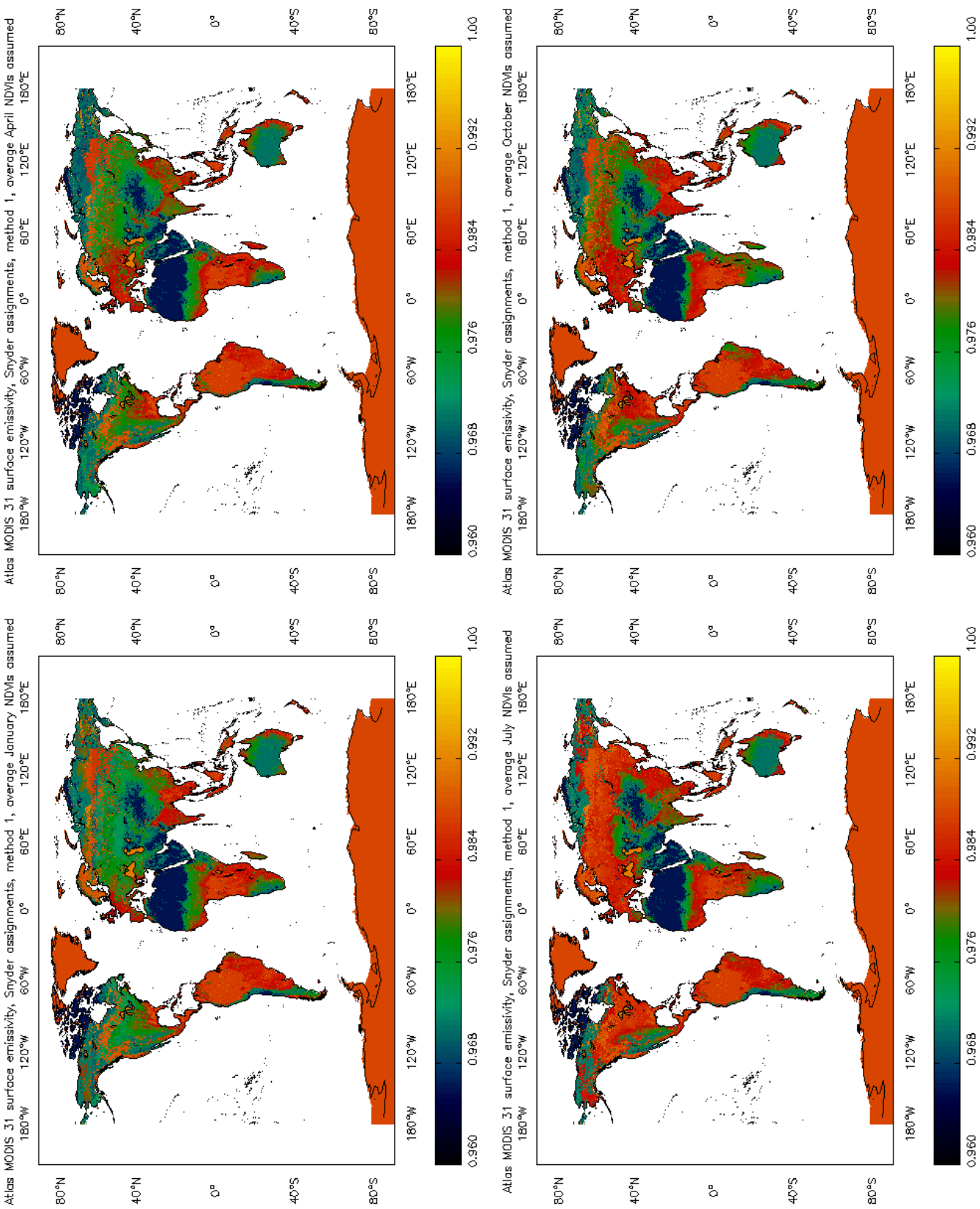

Figure 4: Global plots of land surface emissivity for MODIS band 31 (11.0 μm), for the months of January, April, July and October, as predicted by Method 1.

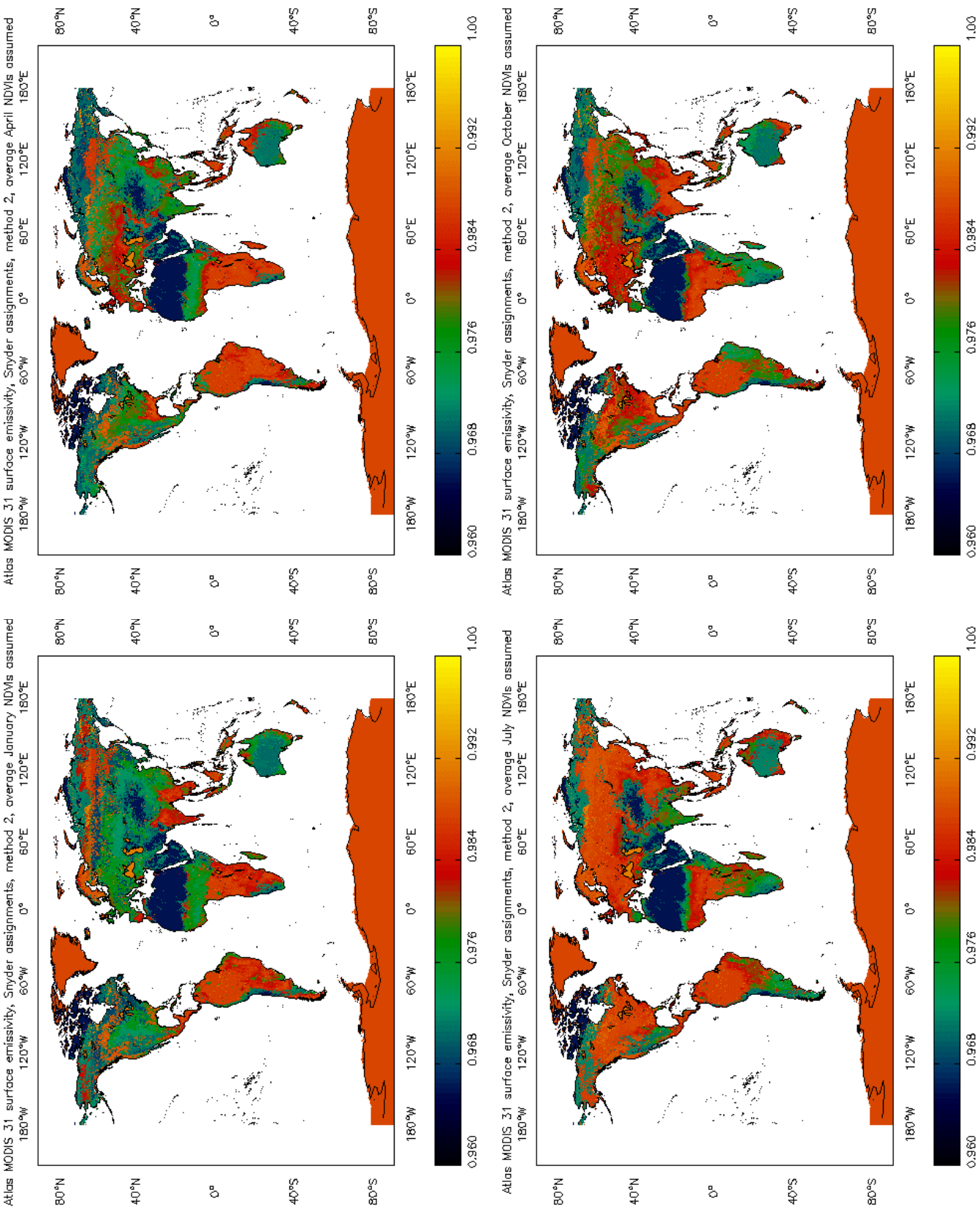

Figure 5: As for Figure 4, but using Method 2.

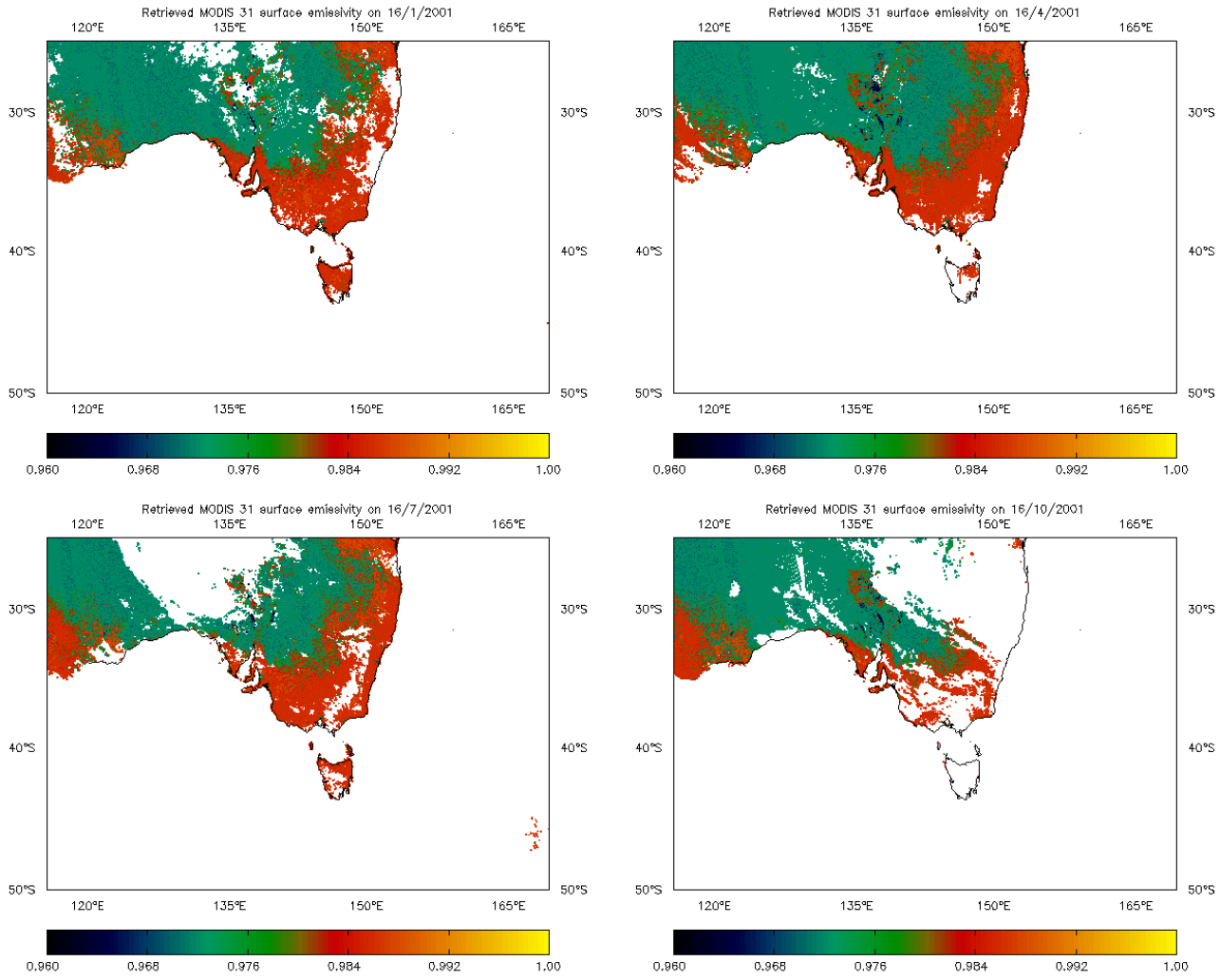

Figure 6: MOD11_L2 band 31 surface emissivity products for south eastern Australia, for 16/1/2001, 16/4/2001, 16/7/2001 and 16/10/2001.

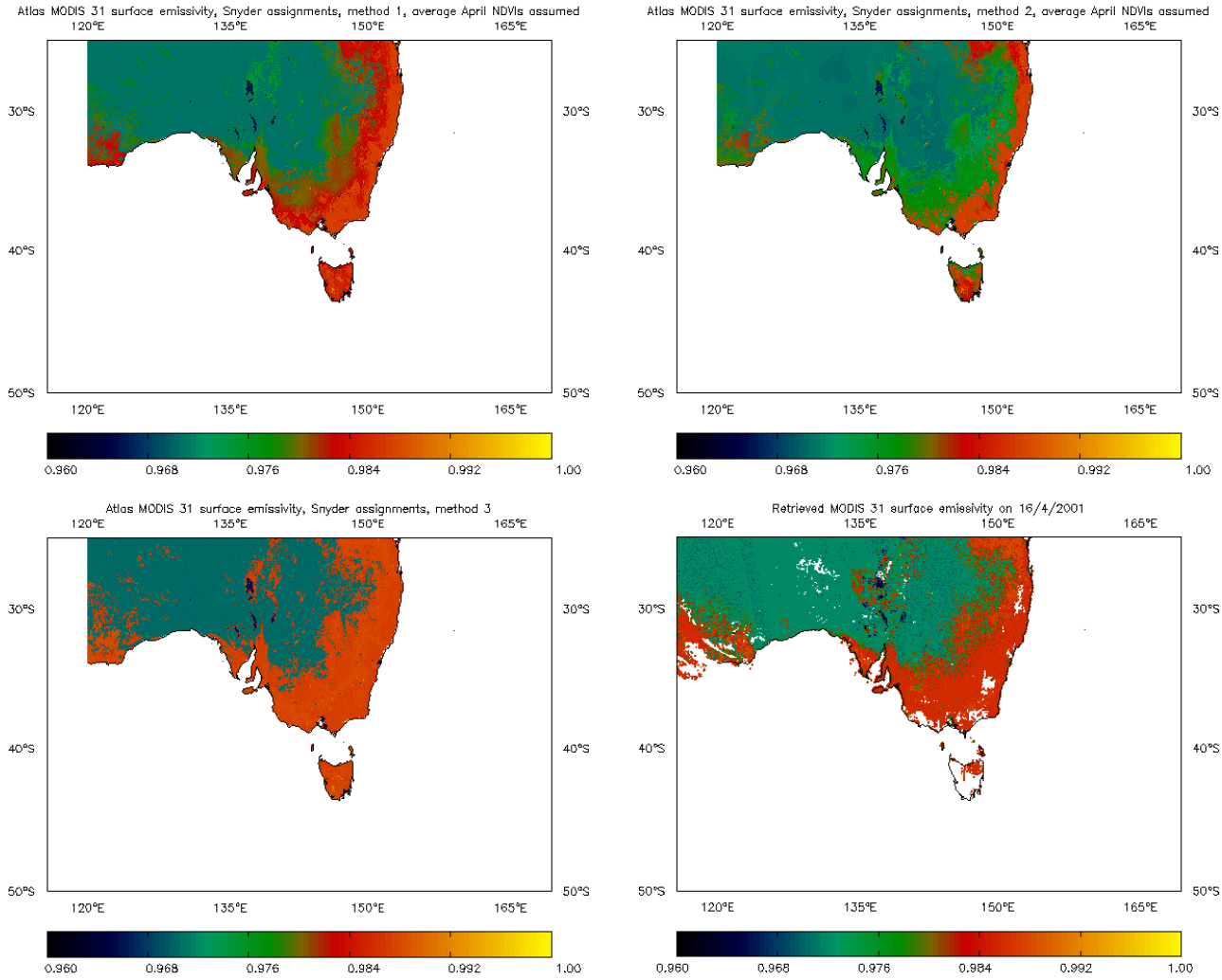

Figure 7: Comparison between the band 31 land surface emissivity values predicted for April by the first three methods outlined in the text with MOD11_L2 data from 16/4/2001.

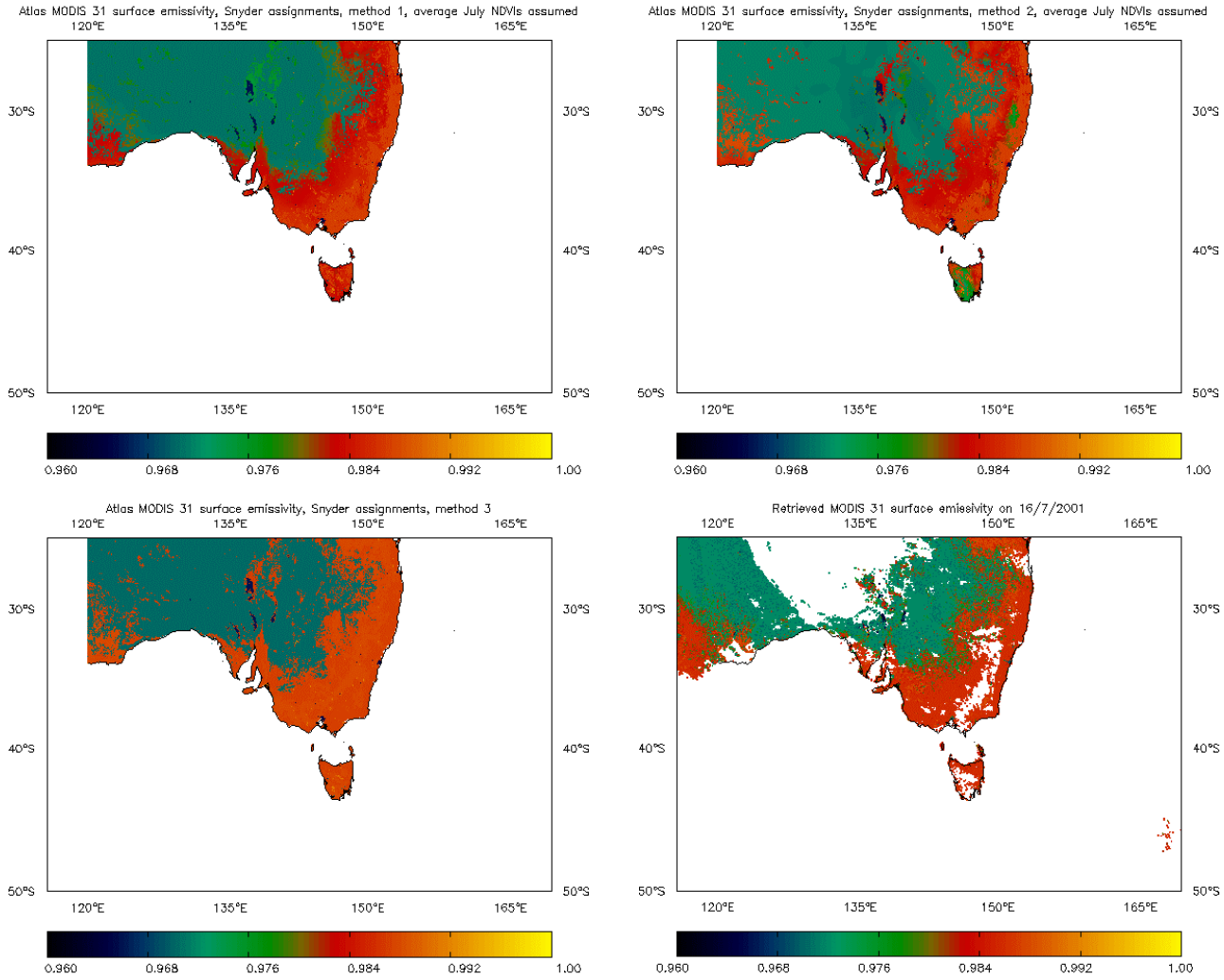

Figure 8: Comparison between the band 31 land surface emissivity values predicted for July by the first three methods outlined in the text with MOD11_L2 data from 16/7/2001.

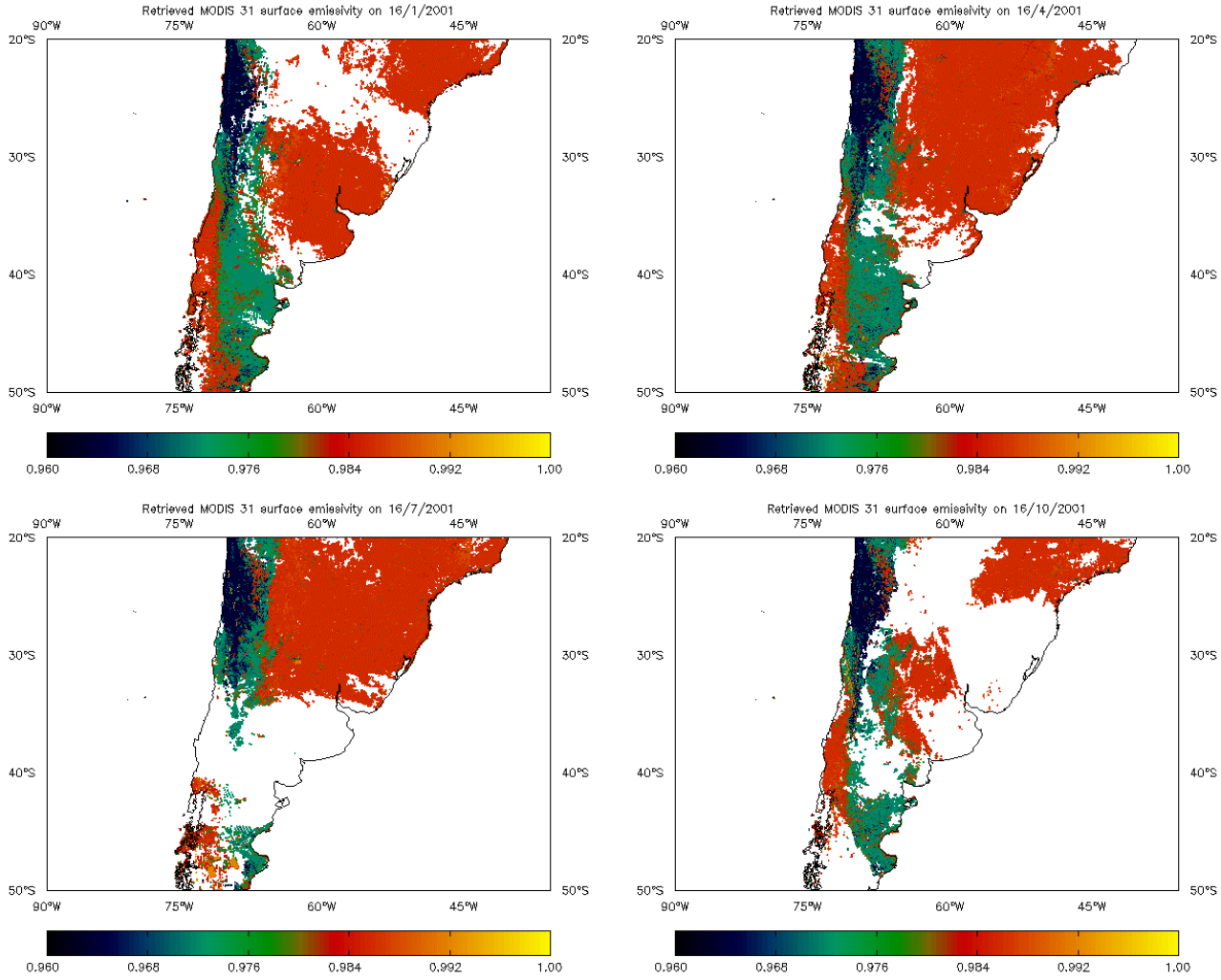

Figure 9: MOD11_L2 band 31 surface emissivity products for central South America, for 16/1/2001, 16/4/2001, 16/7/2001 and 16/10/2001.

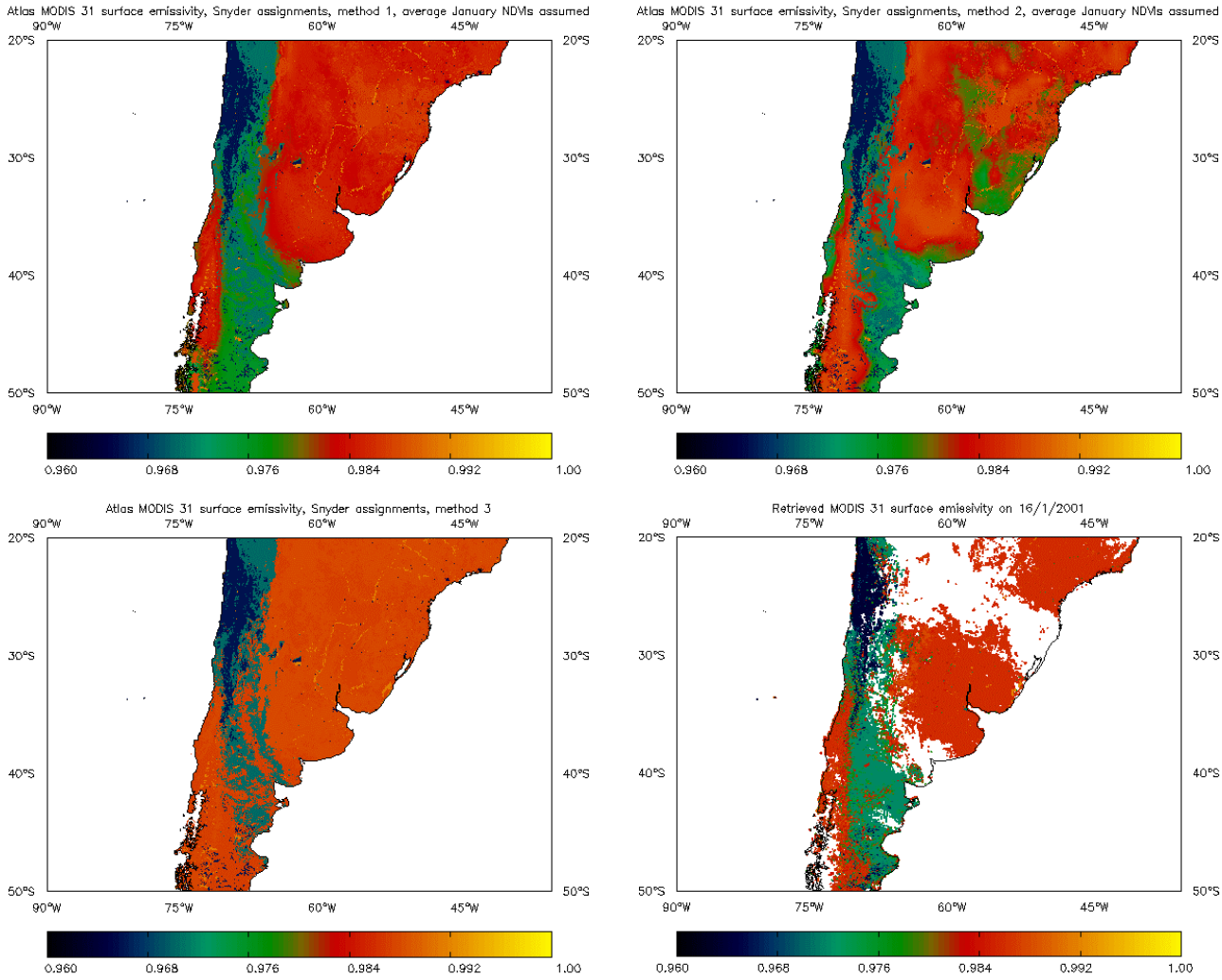

Figure 10: Comparison between the band 31 land surface emissivity values predicted for January by the first three methods outlined in the text with MOD11_L2 data from 16/1/2001.

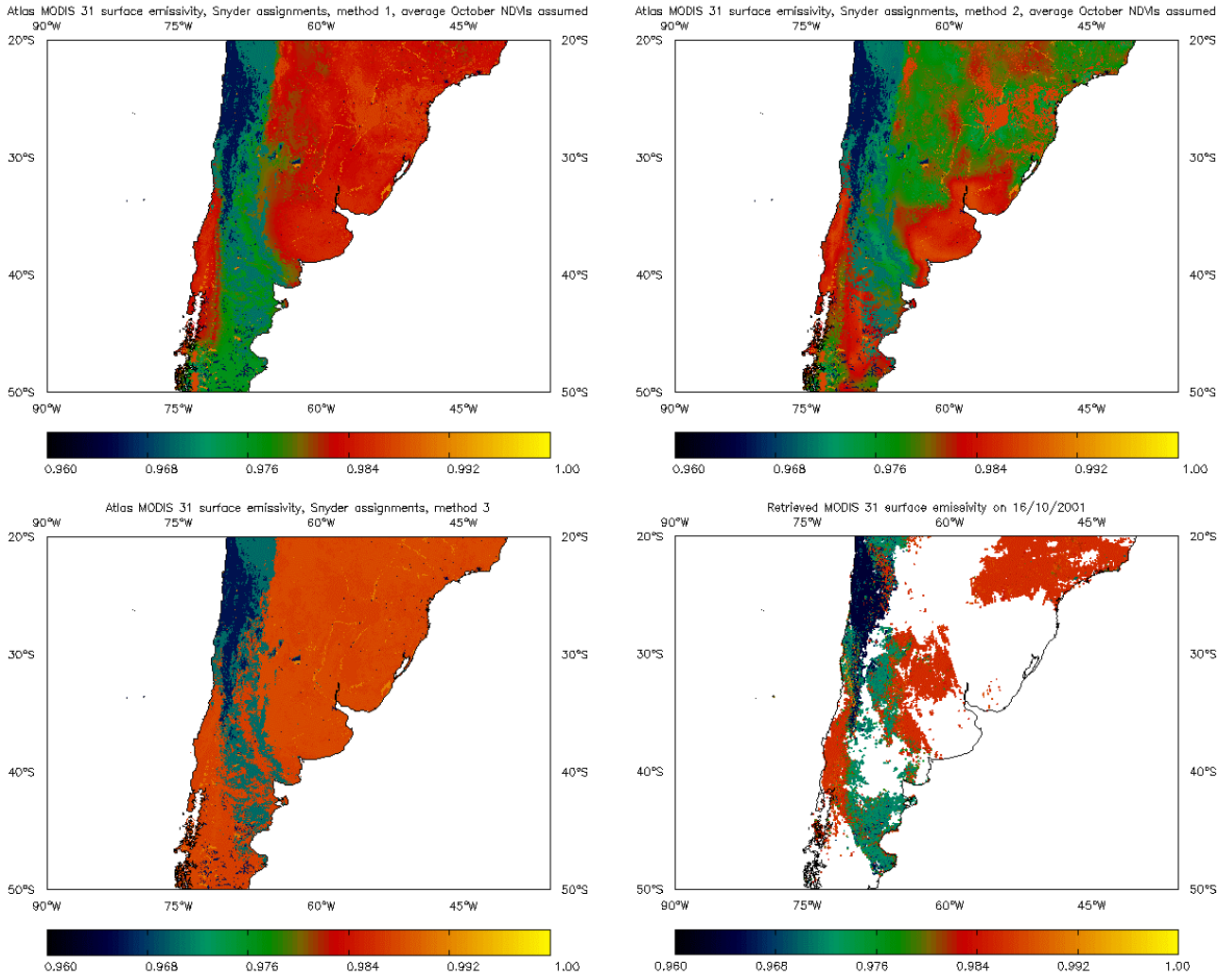

Figure 11: Comparison between the band 31 land surface emissivity values predicted for October by the first three methods outlined in the text with MOD11_L2 data from 16/10/2001.

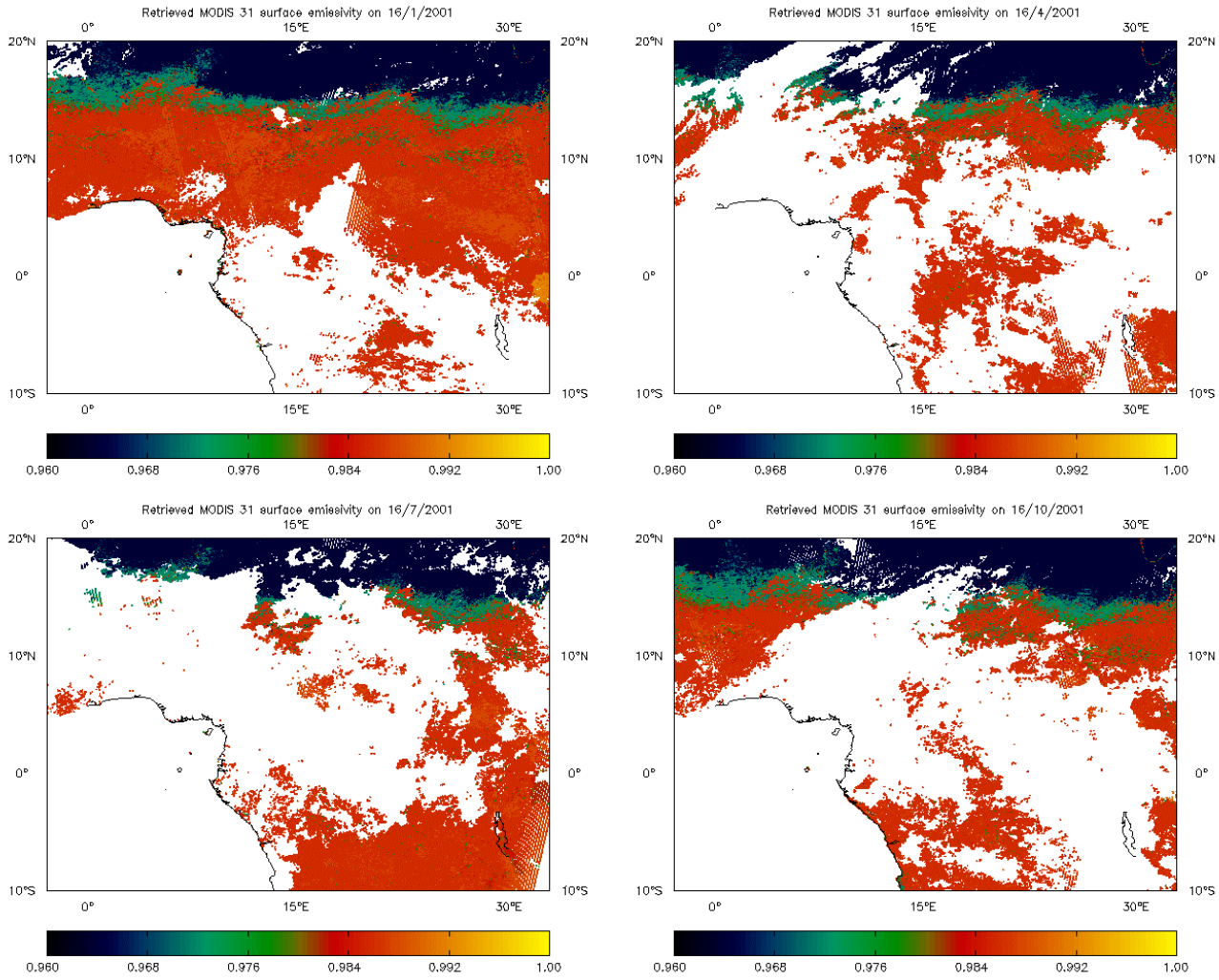

Figure 12: MOD11_L2 band 31 surface emissivity products for central Africa, for 16/1/2001, 16/4/2001, 16/7/2001 and 16/10/2001.

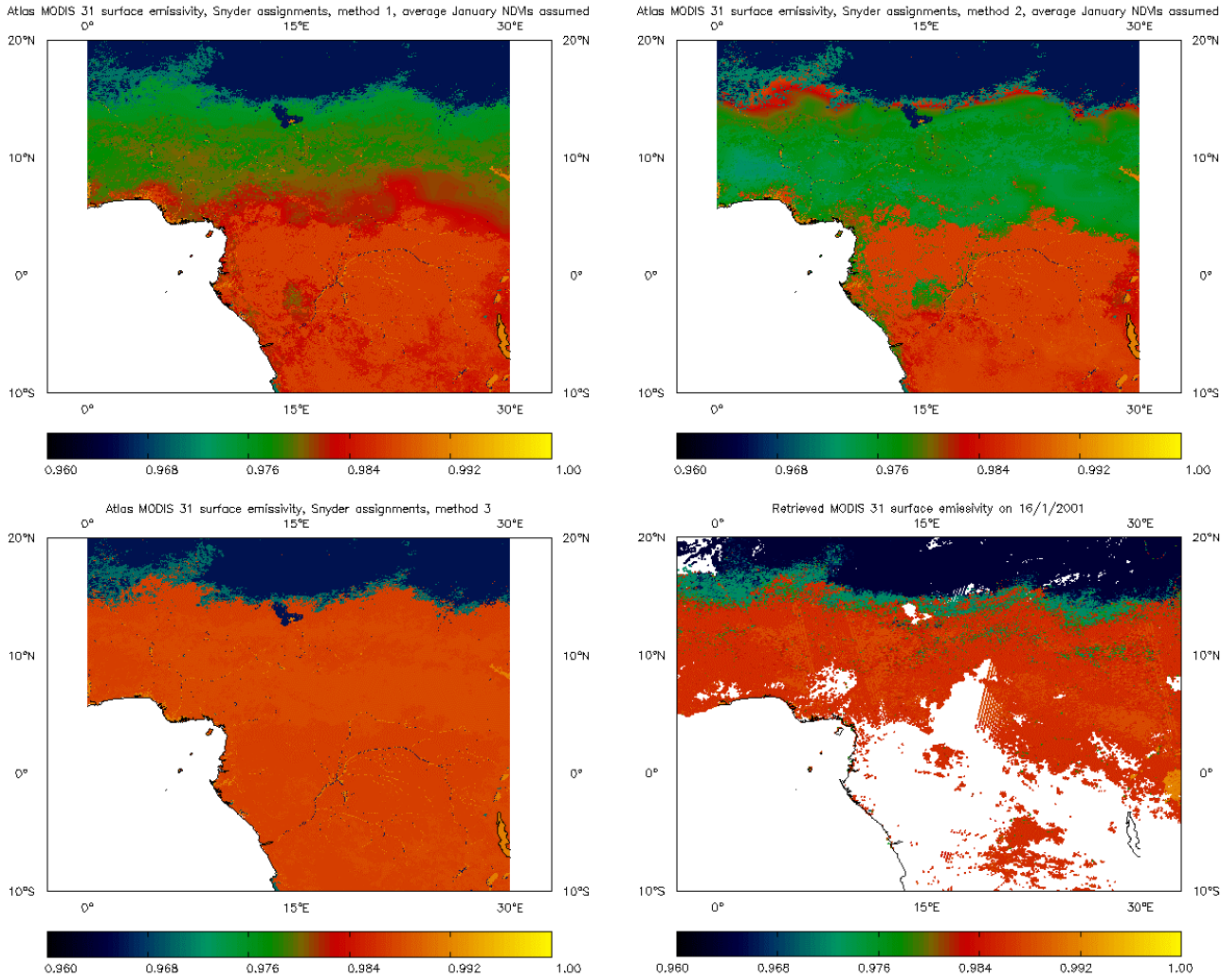

Figure 13: Comparison between the band 31 land surface emissivity values predicted for January by the first three methods outlined in the text with MOD11_L2 data from 16/1/2001.

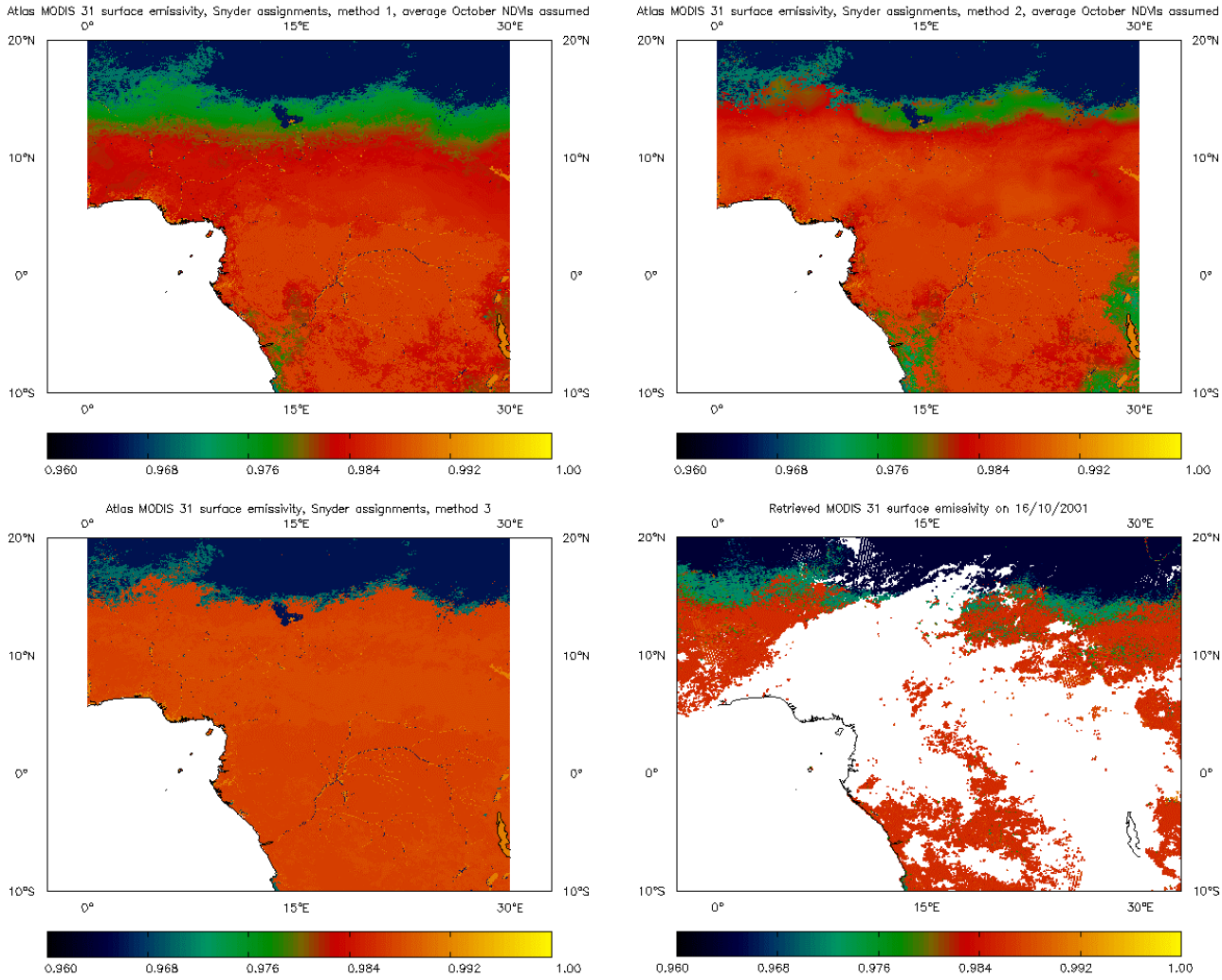

Figure 14: Comparison between the band 31 land surface emissivity values predicted for October by the first three methods outlined in the text with MOD11_L2 data from 16/10/2001.

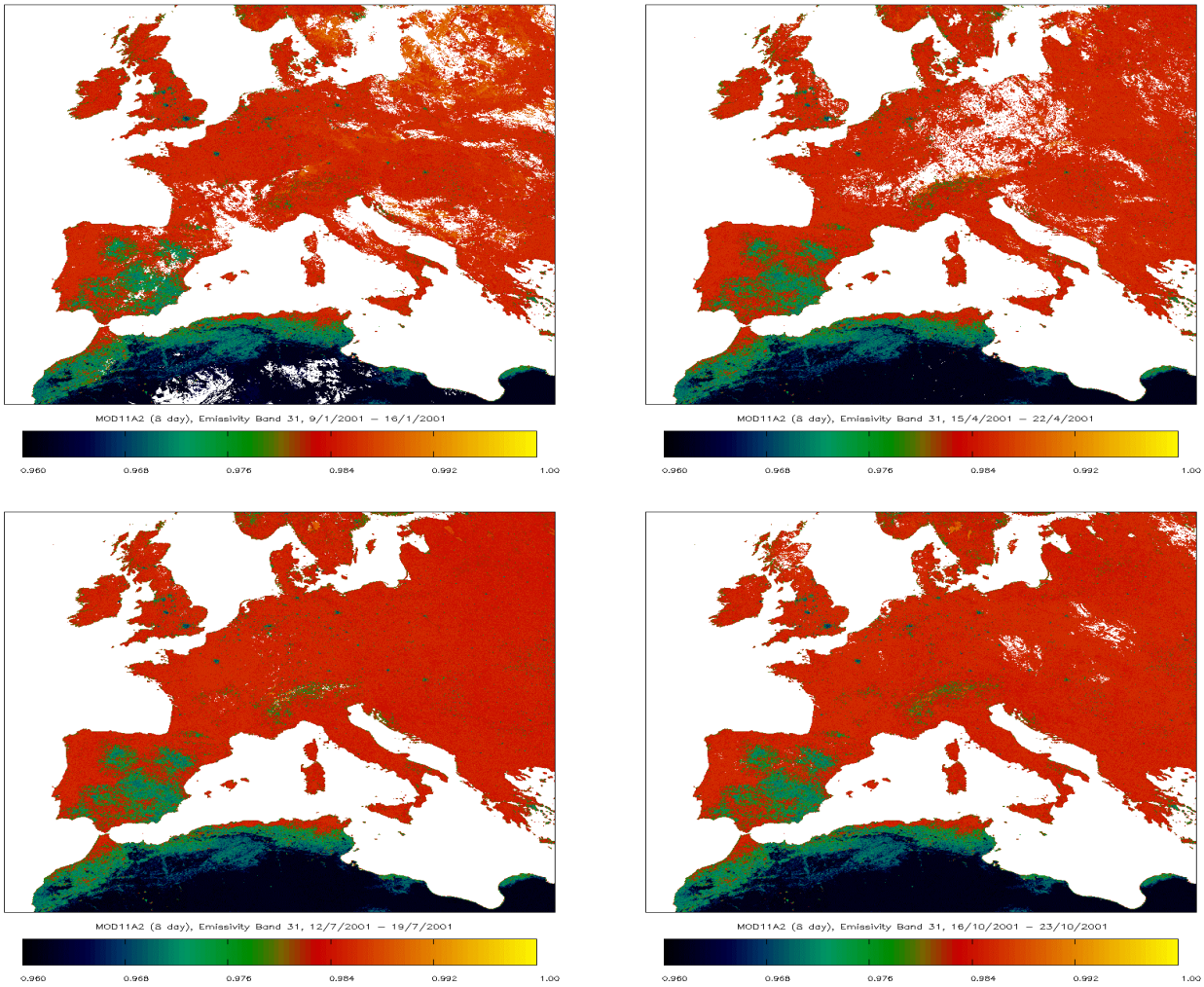

Figure 15: MOD11A2 band 31 surface emissivity products for western Europe, for 16/1/2001, 16/4/2001, 16/7/2001 and 16/10/2001.

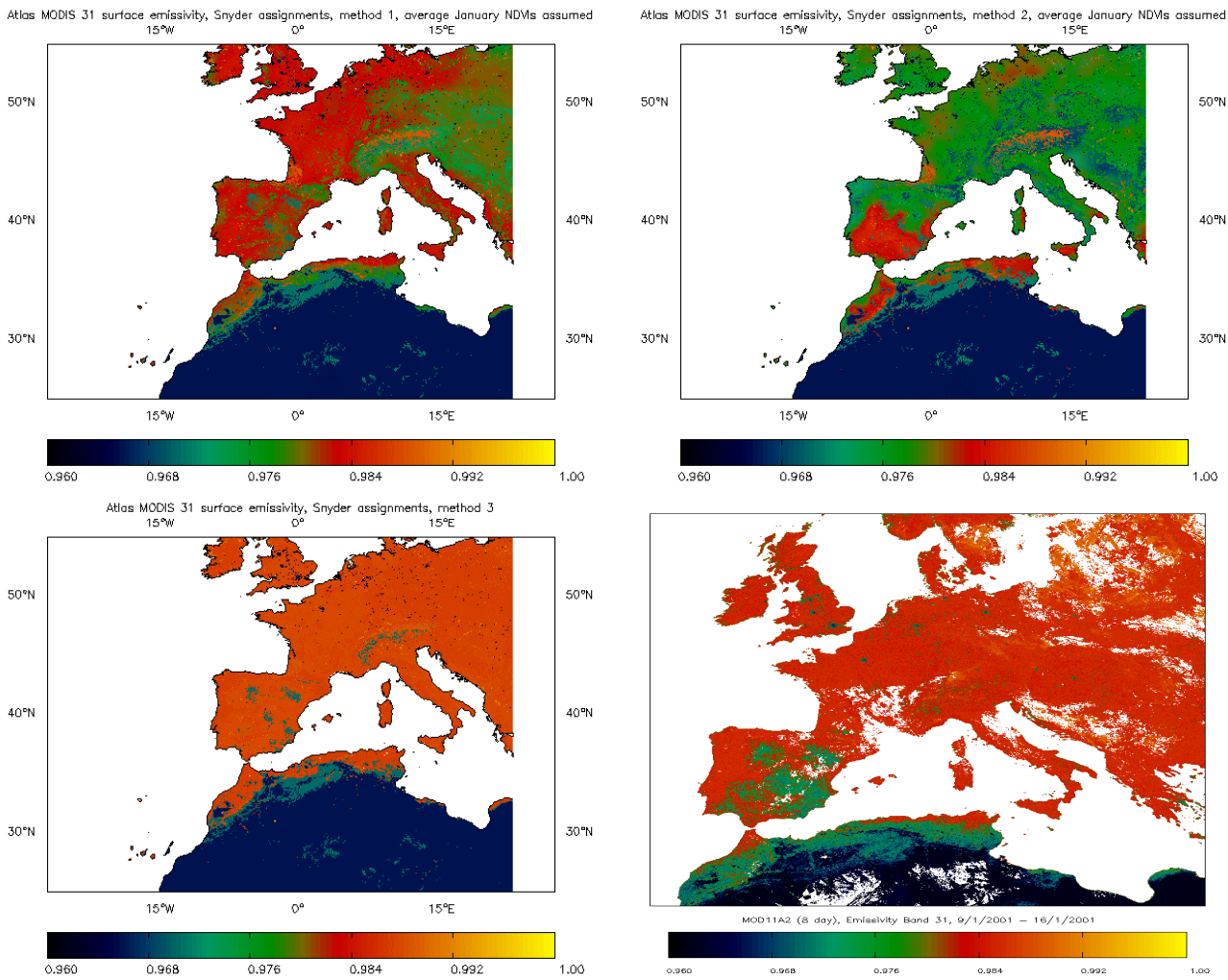

Figure 16: Comparison between the band 31 land surface emissivity values predicted for January by the first three methods outlined in the text with MOD11A2 data from 16/1/2001.

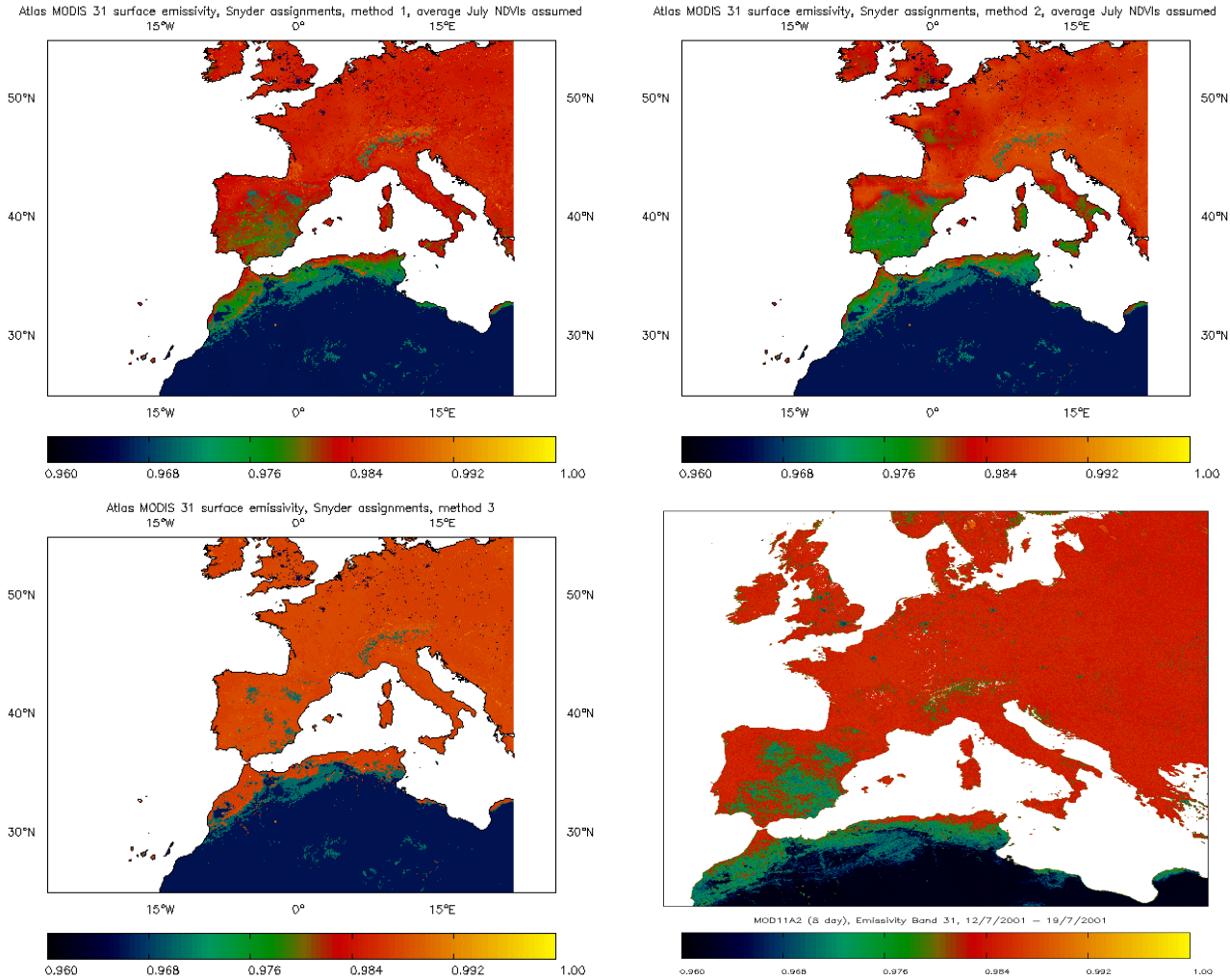

Figure 17: Comparison between the band 31 land surface emissivity values predicted for July by the first three methods outlined in the text with MOD11A2 data from 16/7/2001.

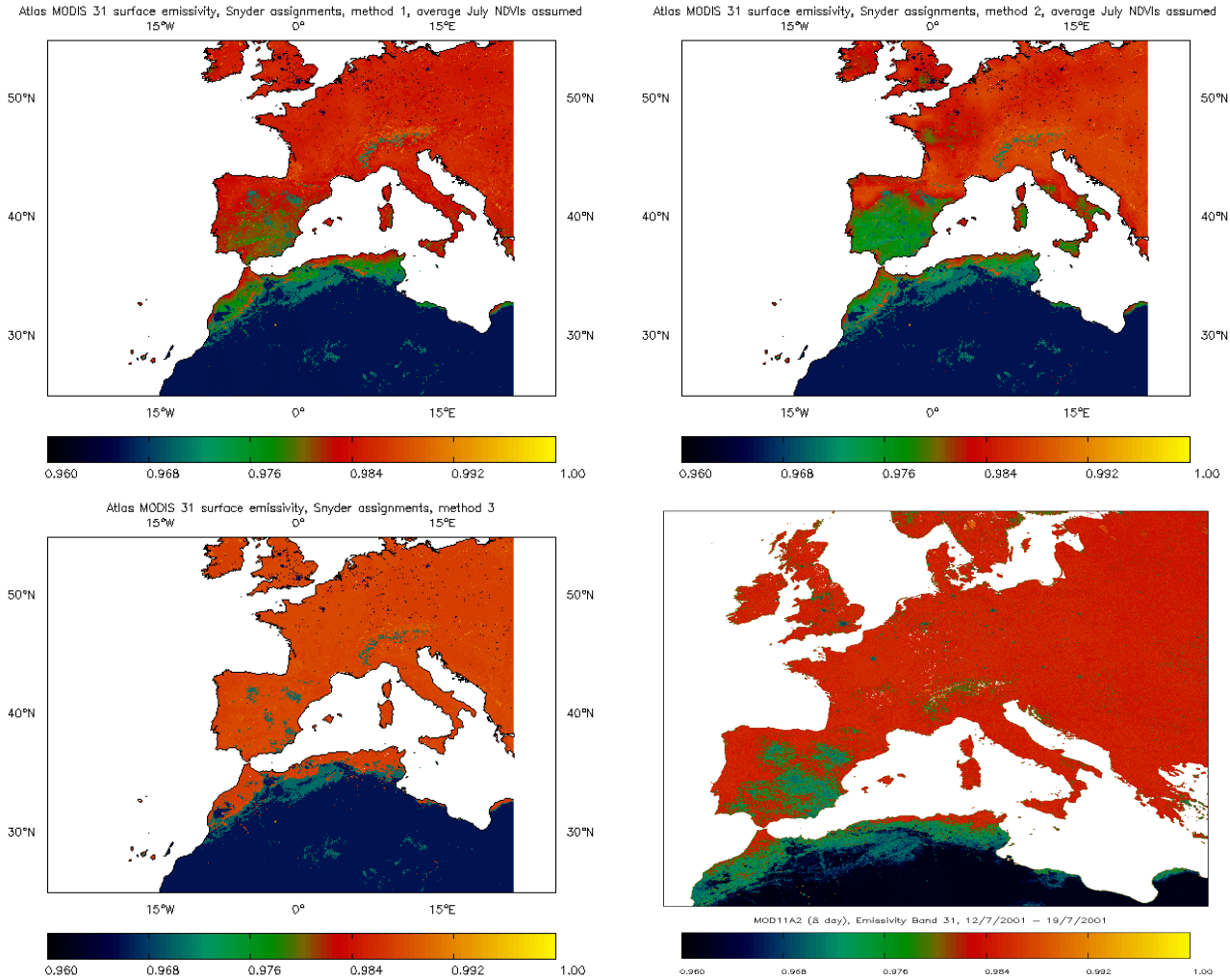

Figure 17: Comparison between the band 31 land surface emissivity values predicted for July by the first three methods outlined in the text with MOD11A2 data from 16/7/2001.

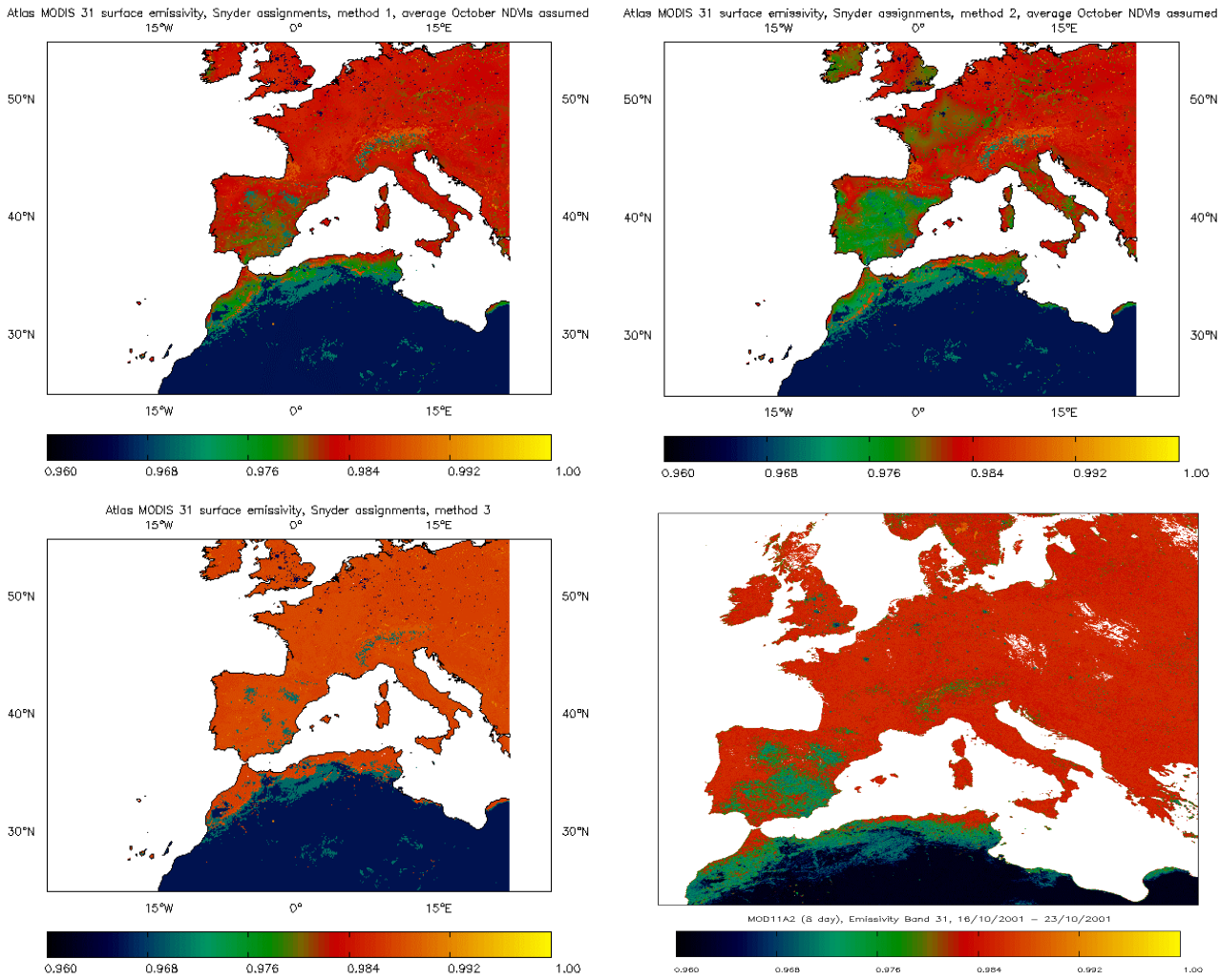

Figure 18: Comparison between the band 31 land surface emissivity values predicted for October by the first three methods outlined in the text with MOD11A2 data from 16/10/2001.

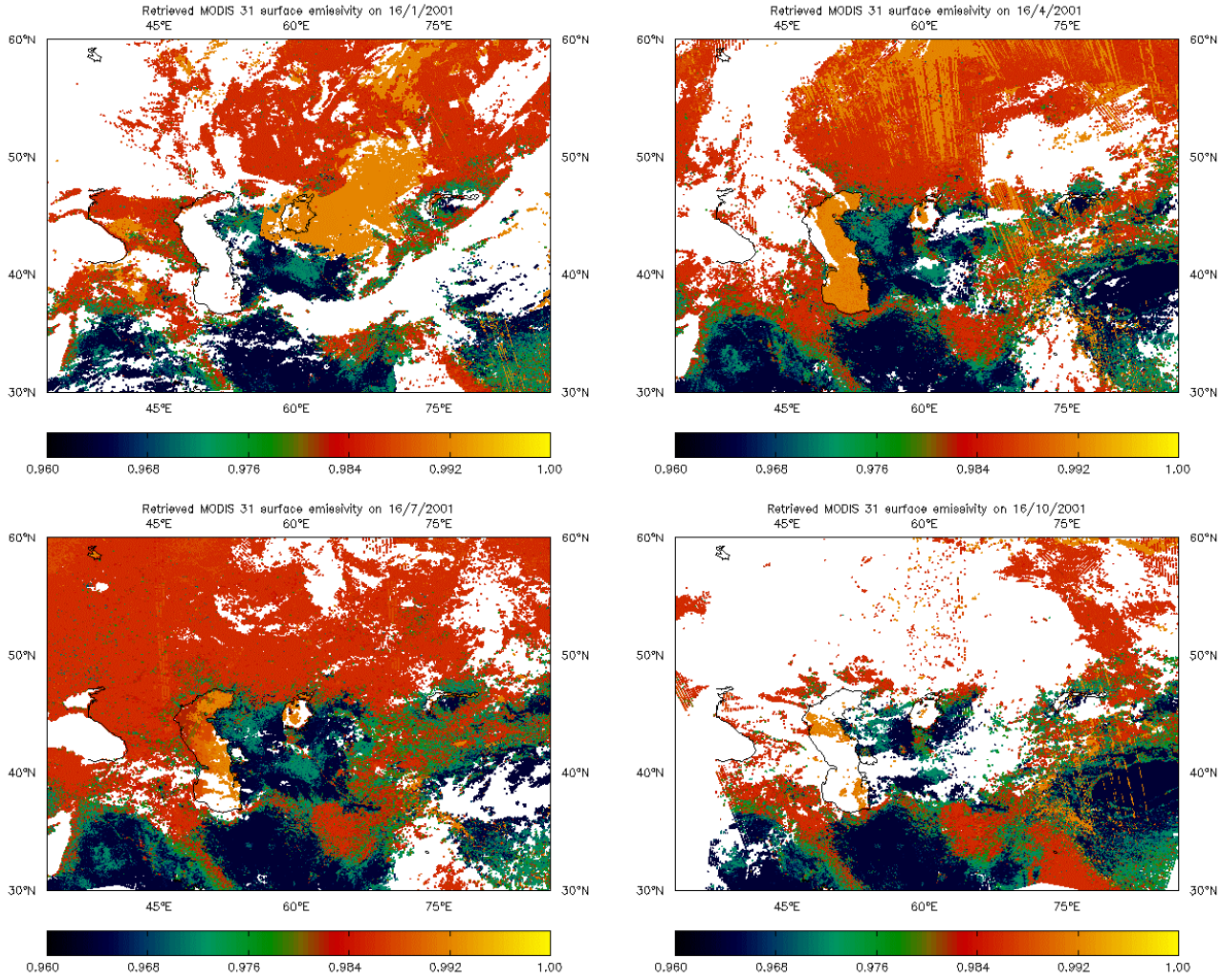

Figure 19: MOD11_L2 band 31 surface emissivity products for central Asia, for 16/1/2001, 16/4/2001, 16/7/2001 and 16/10/2001.

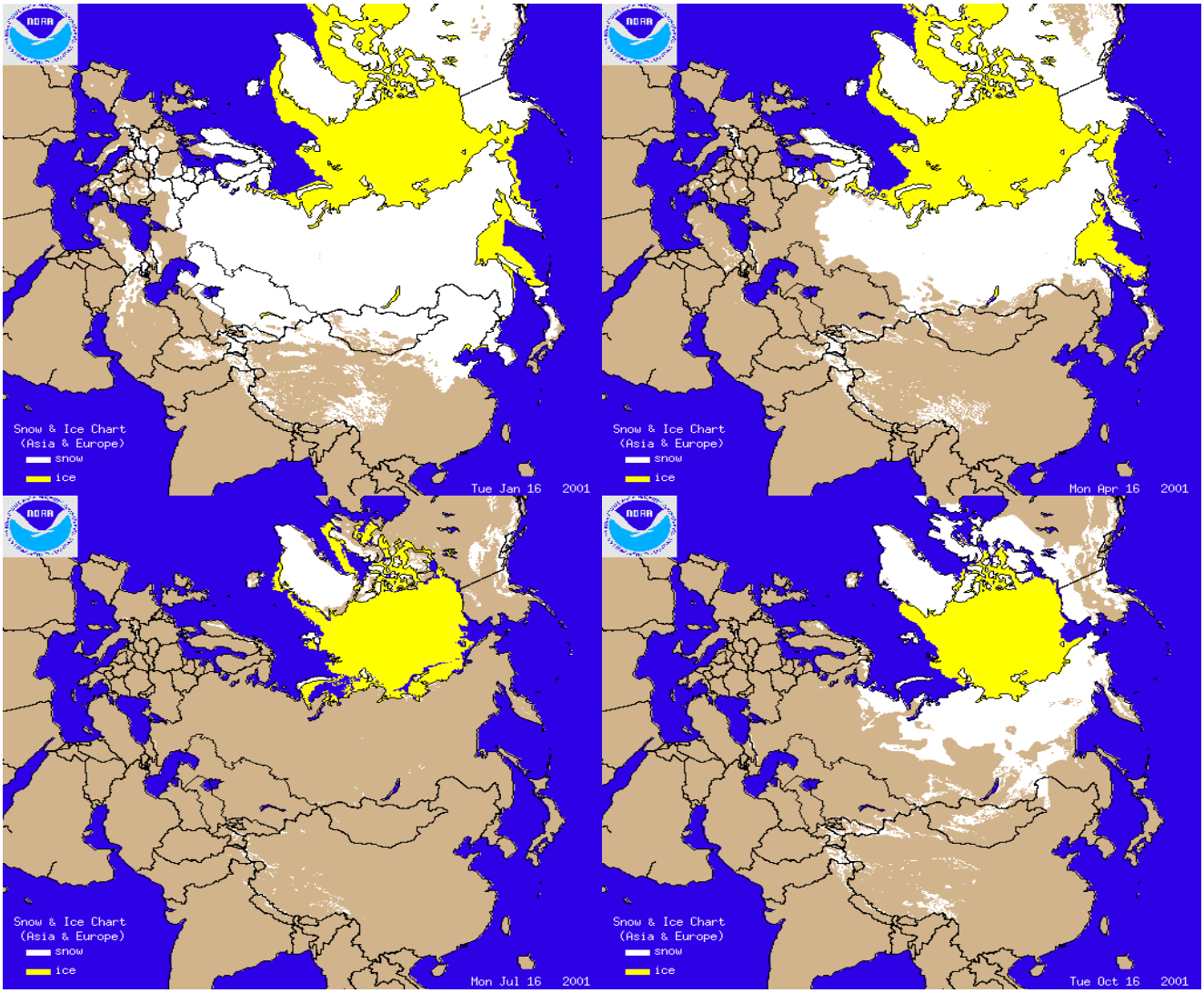

Figure 20: Images from the NESDIS Operational Daily Snow Cover Analysis product for 16/1/2001, 16/4/2001, 16/7/2001 and 16/10/2001.

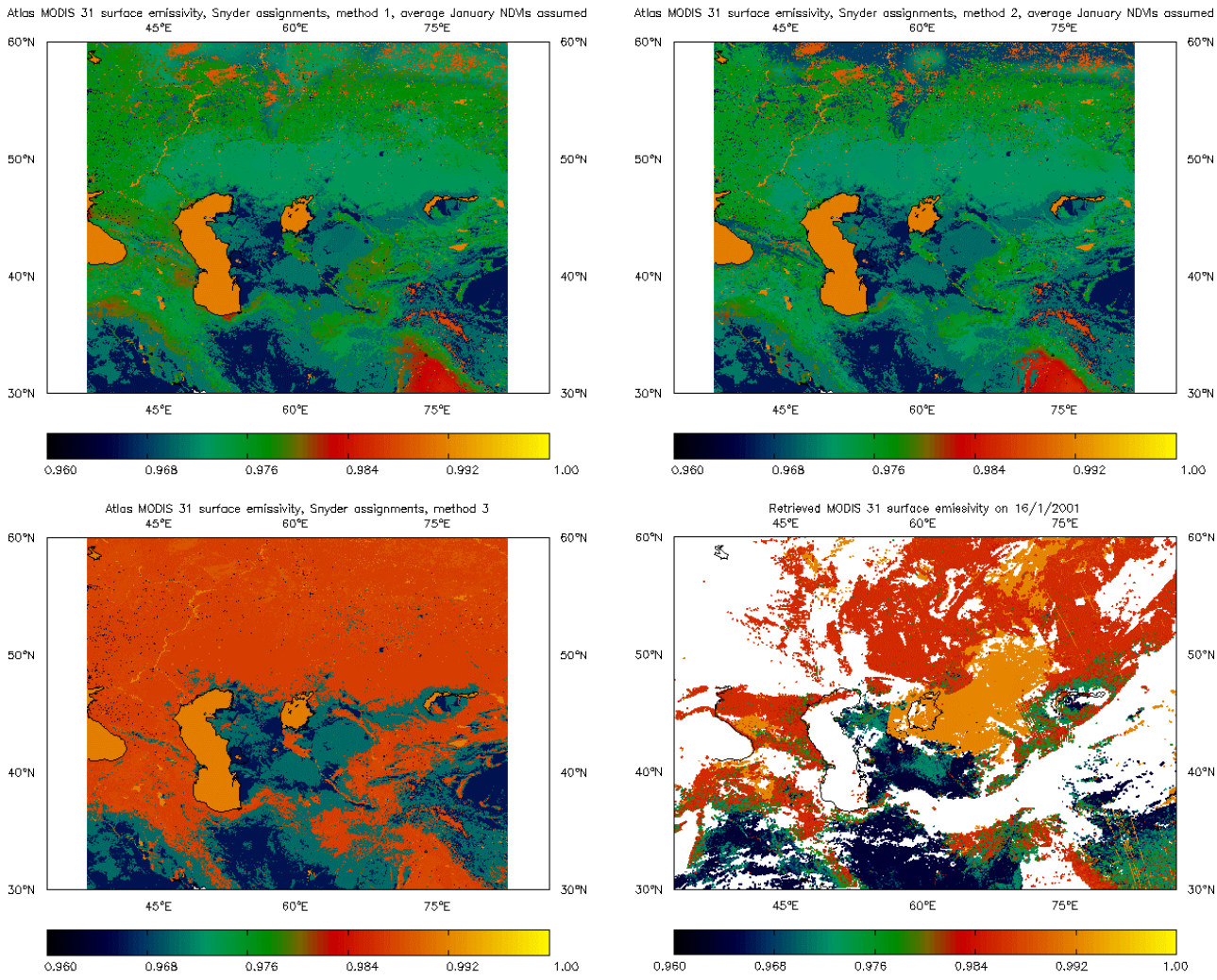

Figure 21: Comparison between the band 31 land surface emissivity values predicted for January by the first three methods outlined in the text with MOD11_L2 data from 16/1/2001.

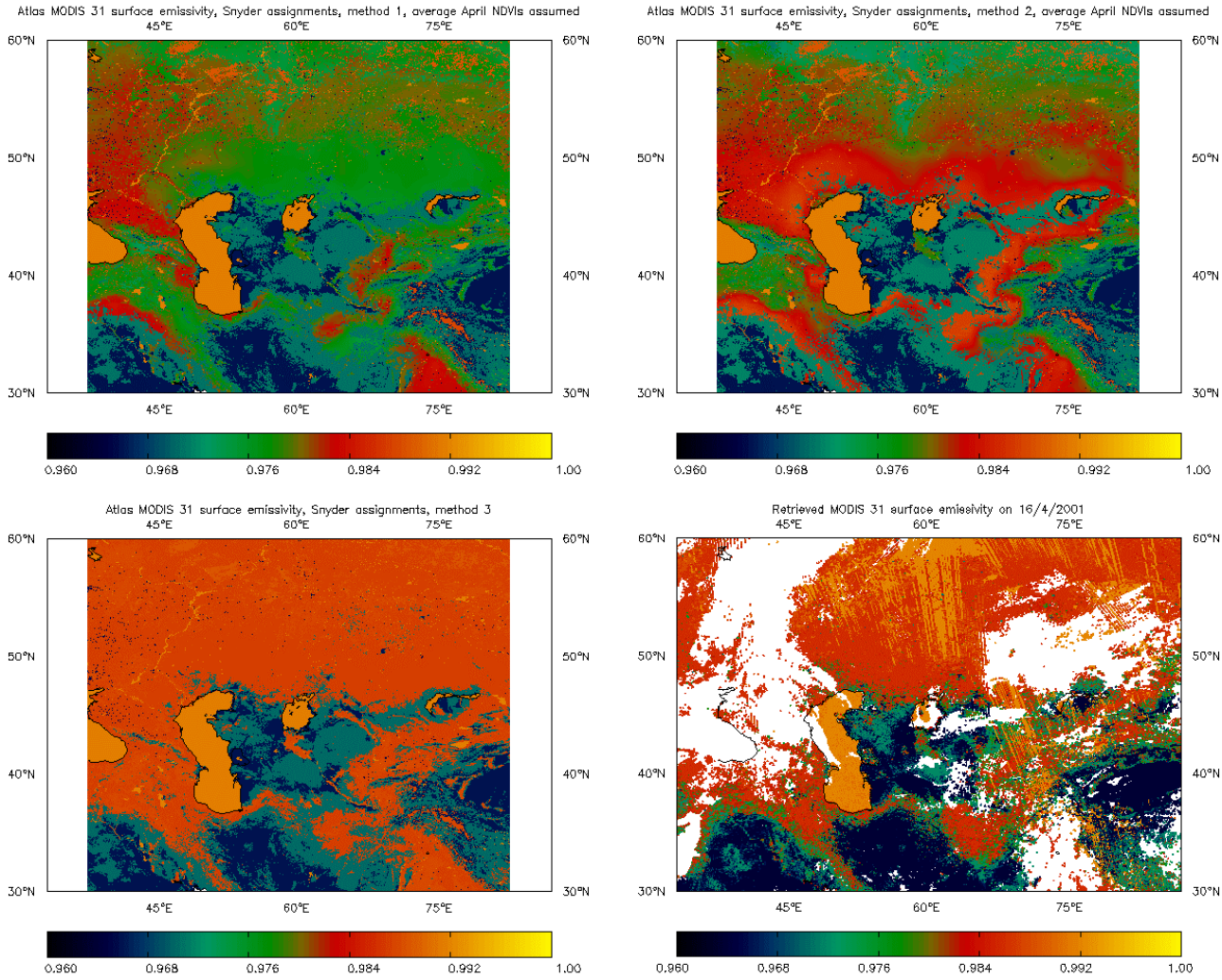

Figure 22: Comparison between the band 31 land surface emissivity values predicted for April by the first three methods outlined in the text with MOD11_L2 data from 16/4/2001.

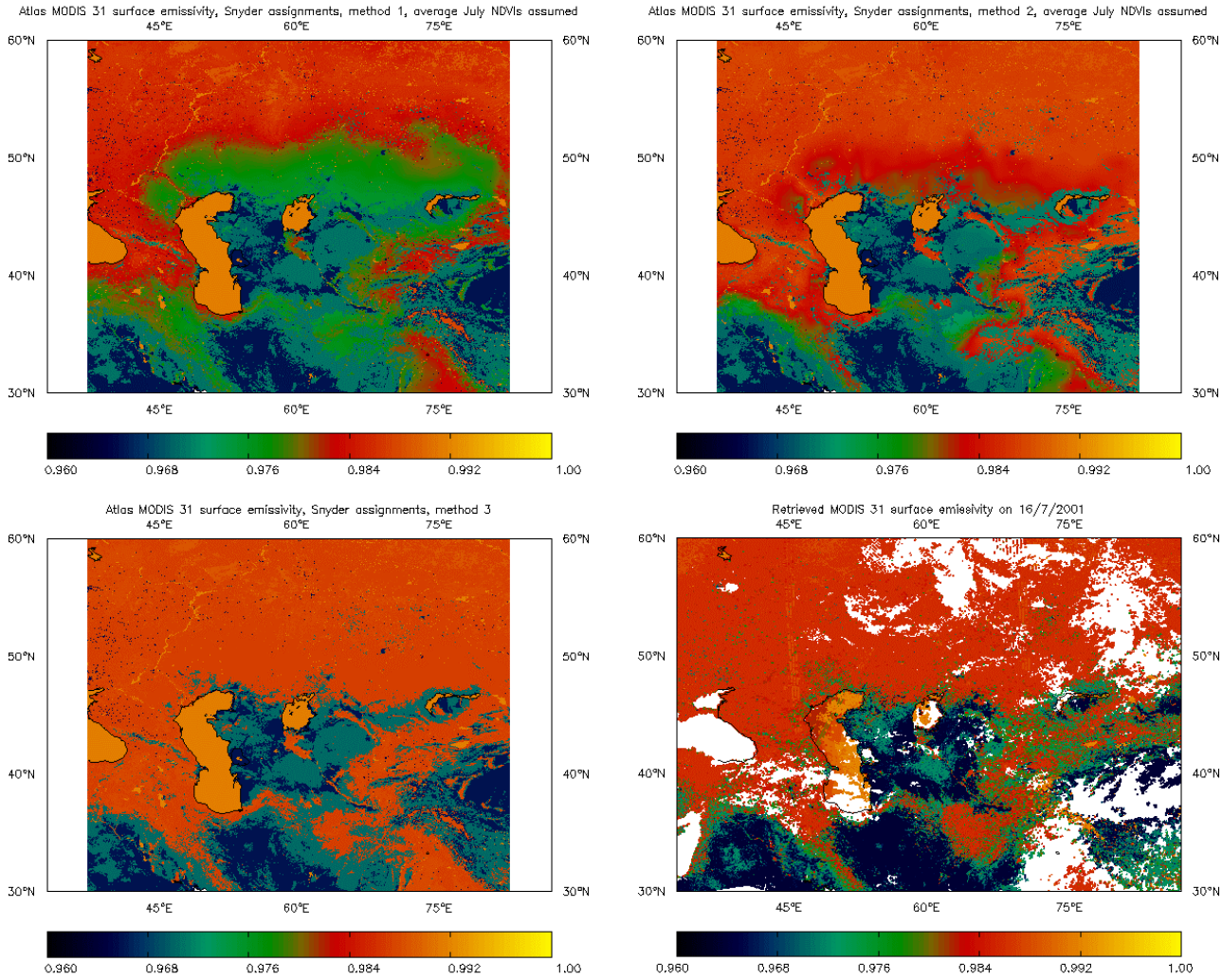

Figure 23: Comparison between the band 31 land surface emissivity values predicted for July by the first three methods outlined in the text with MOD11_L2 data from 16/7/2001.

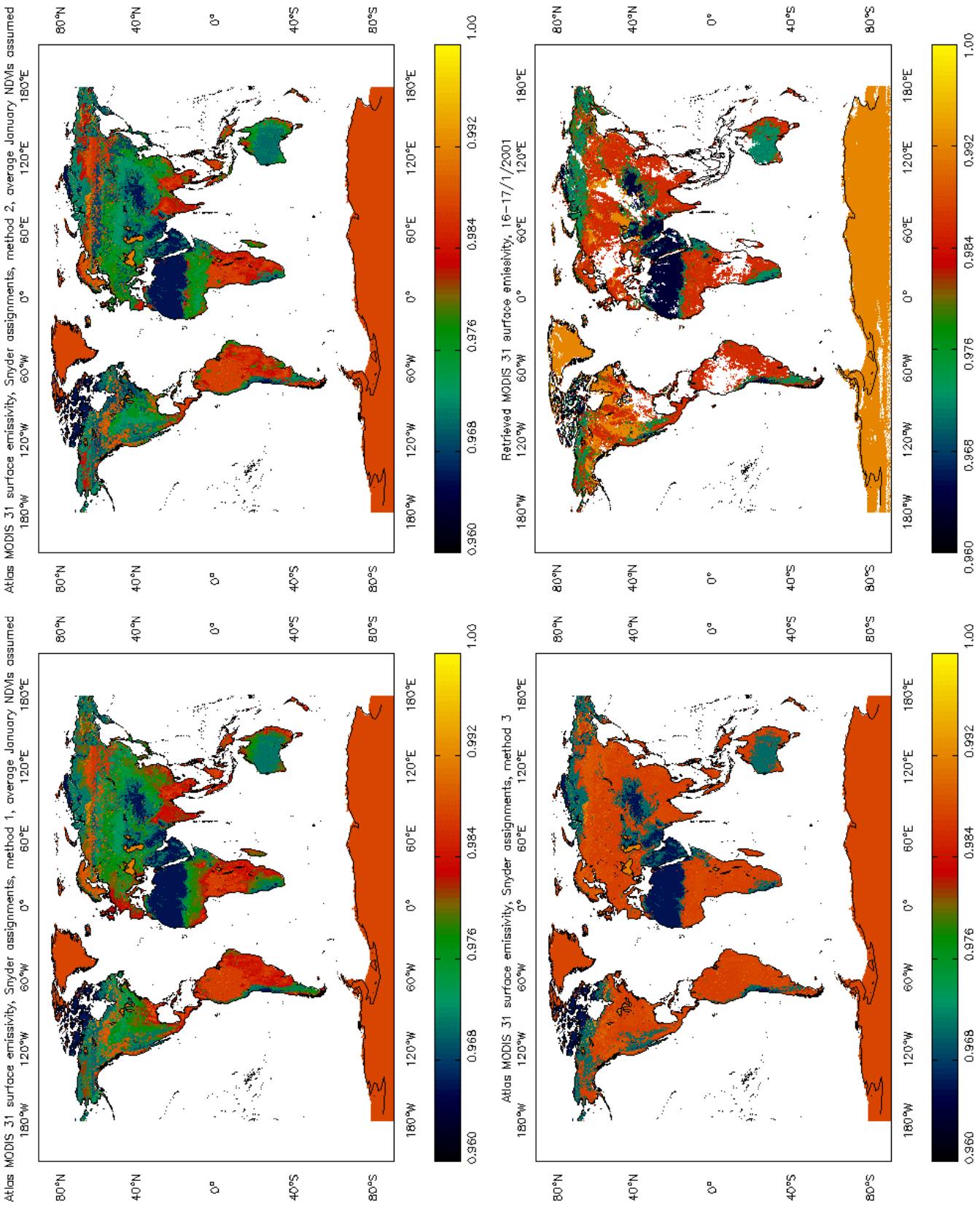

Figure 24: Comparison between the band 31 (11.0 µm) land surface emissivity values predicted for January by the first three methods outlined in the text with MOD11_L2 data from 16 - 17/1/2001.

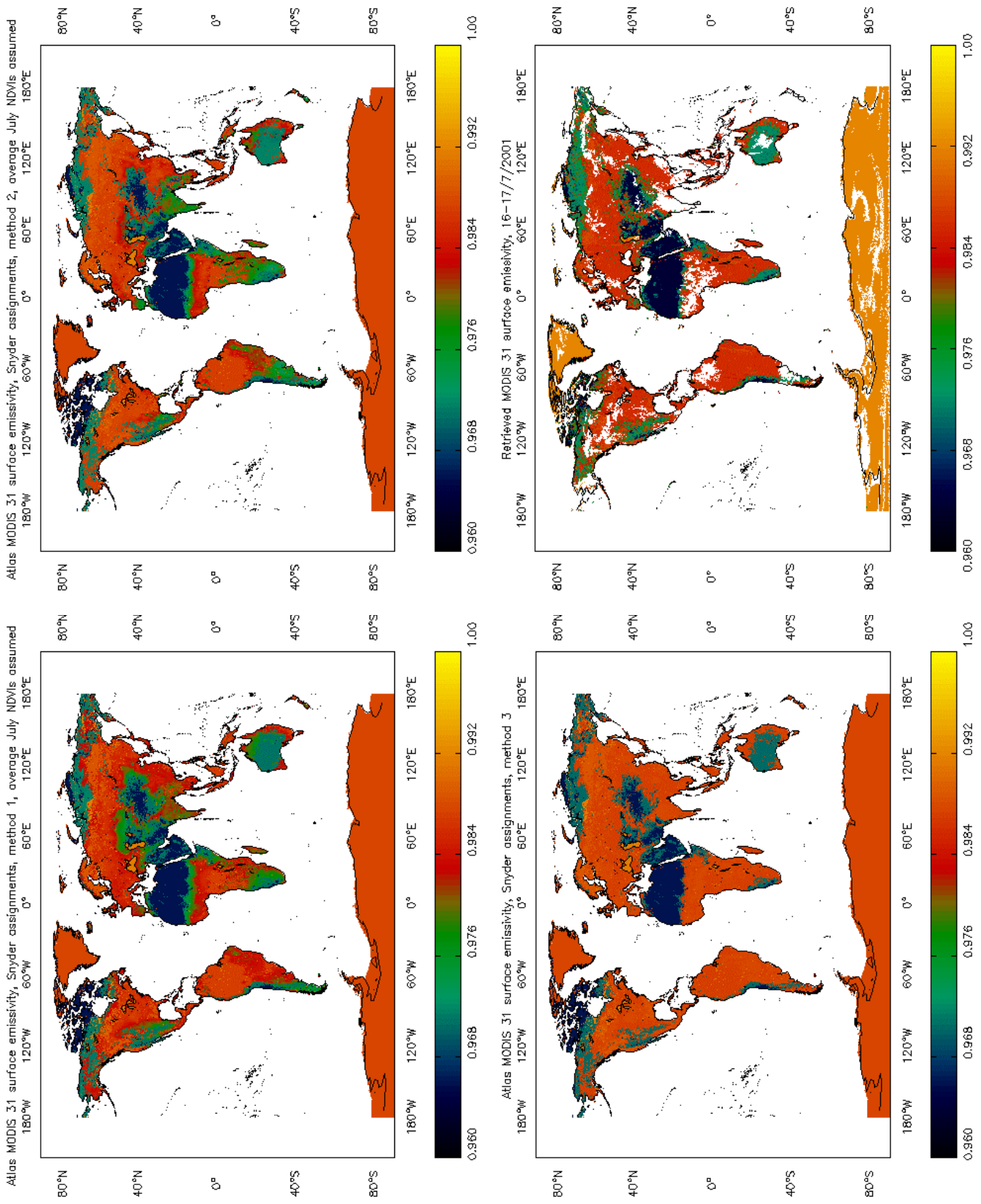

Figure 25: Comparison between the band 31 (11.0 µm) land surface emissivity values predicted for July by the first three methods outlined in the text with MOD11_L2 data from 16 - 17/7/2001.

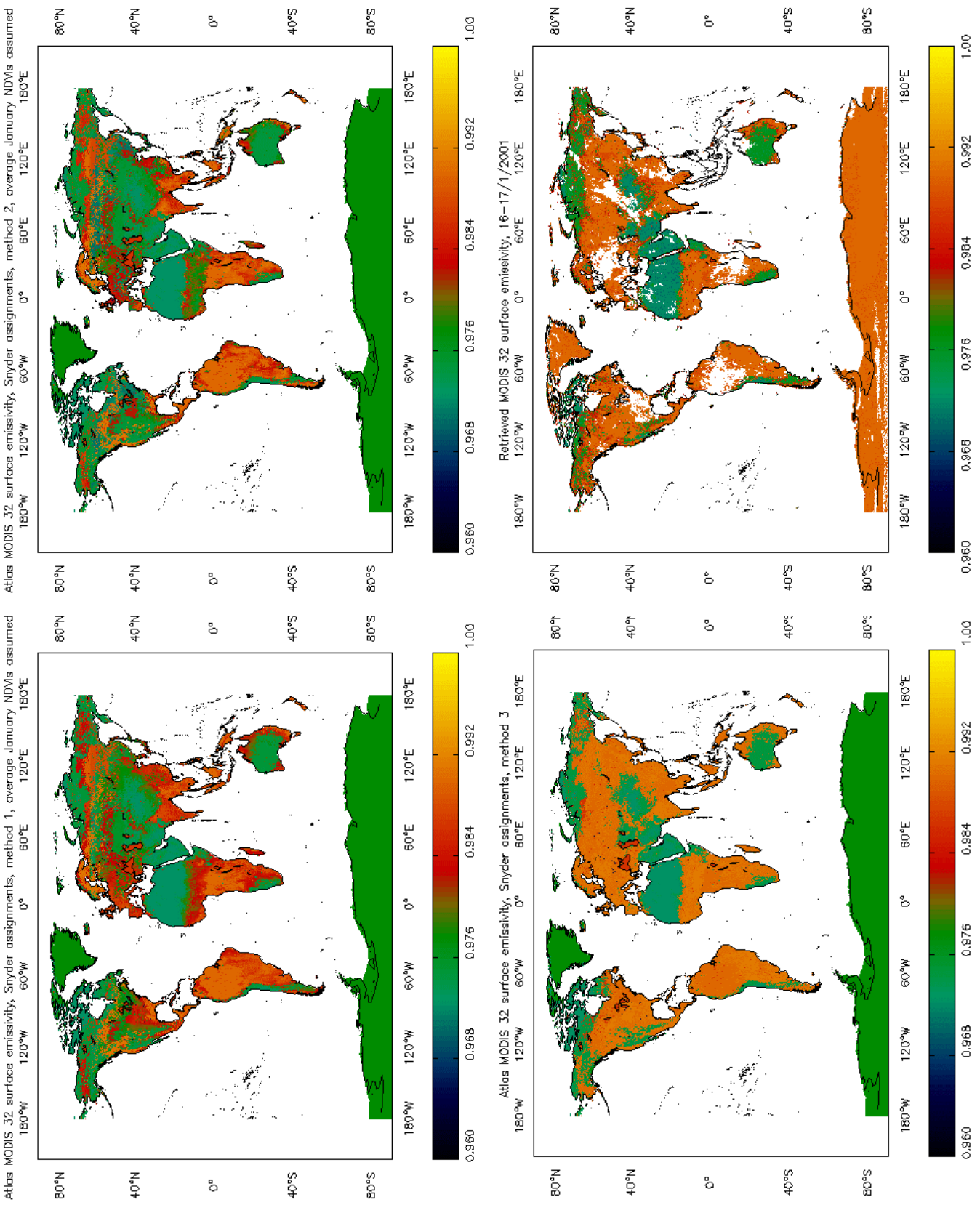

Figure 26: Comparison between the band 32 (12.0 µm) land surface emissivity values predicted for January by the first three methods outlined in the text with MOD11_L2 data from 16 - 17/1/2001.

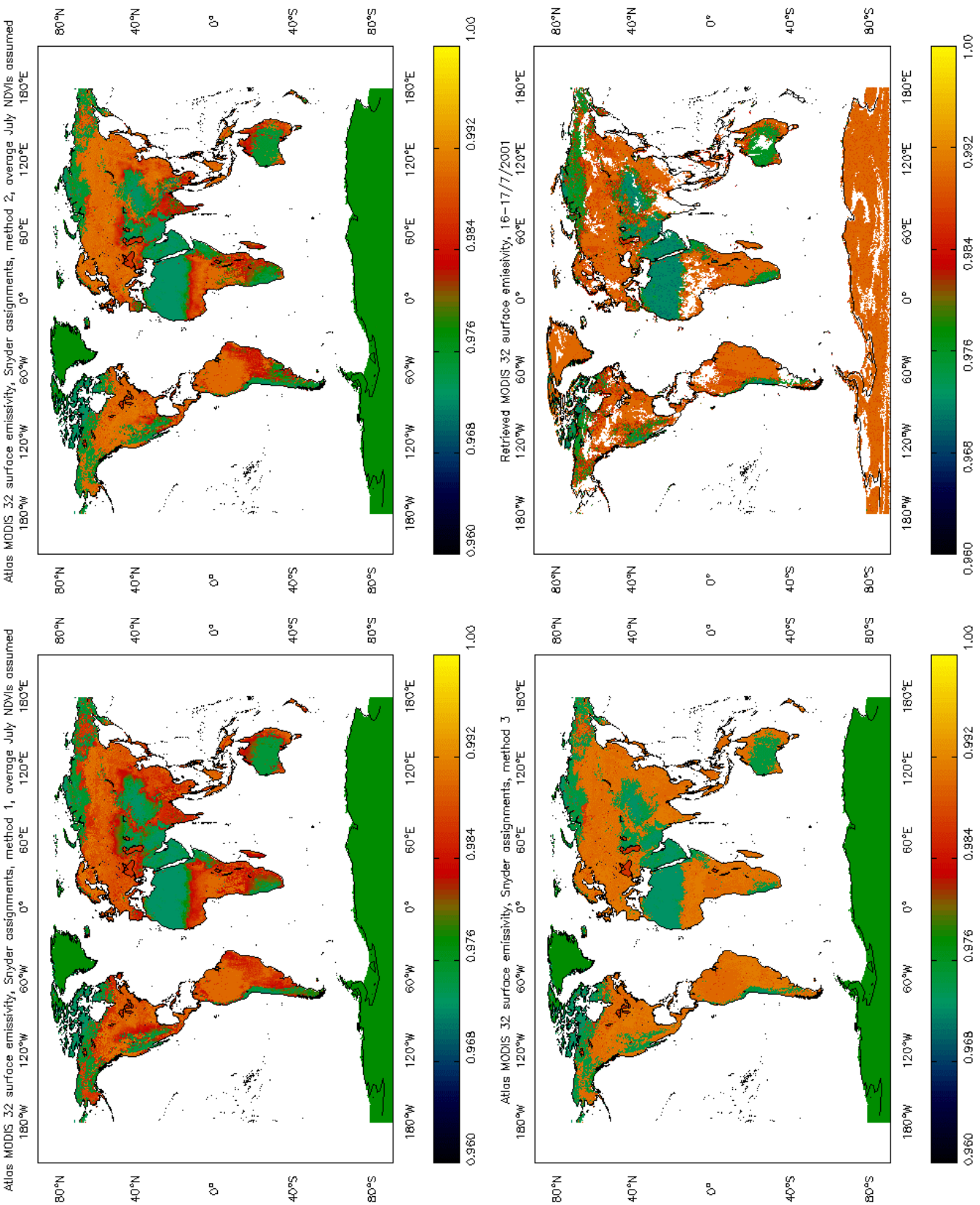

Figure 27: Comparison between the band 32 (12.0 μm) land surface emissivity values predicted for July by the first three methods outlined in the text with MOD11_L2 data from 16 - 17/7/2001.

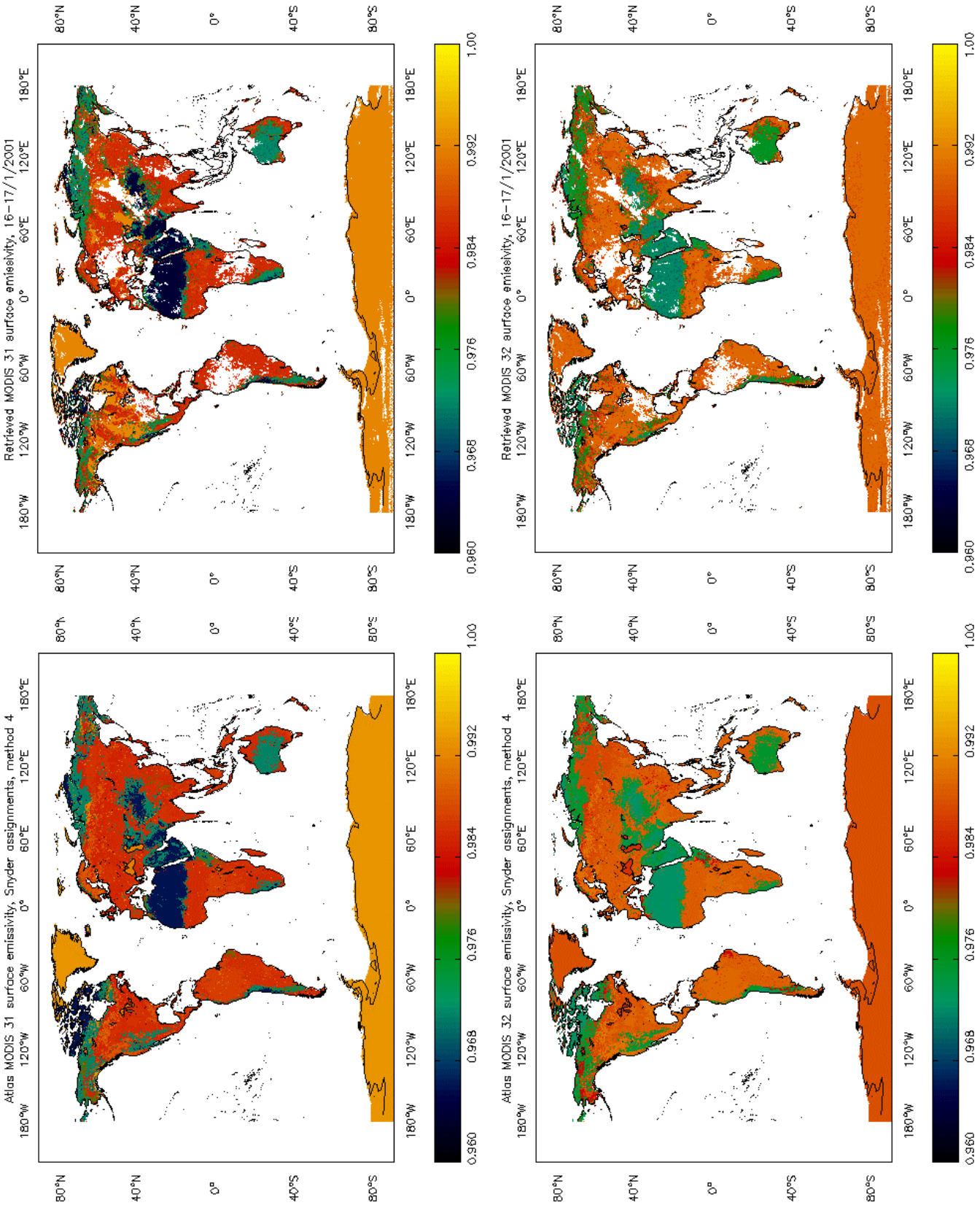

Figure 28: Comparison between band 31 (11.0 μm) and band 32 (12.0 μm) land surface emissivity values for January predicted by the tuned scheme described in the text (Method 4) with MOD11_L2 data from 16 - 17/1/2001.

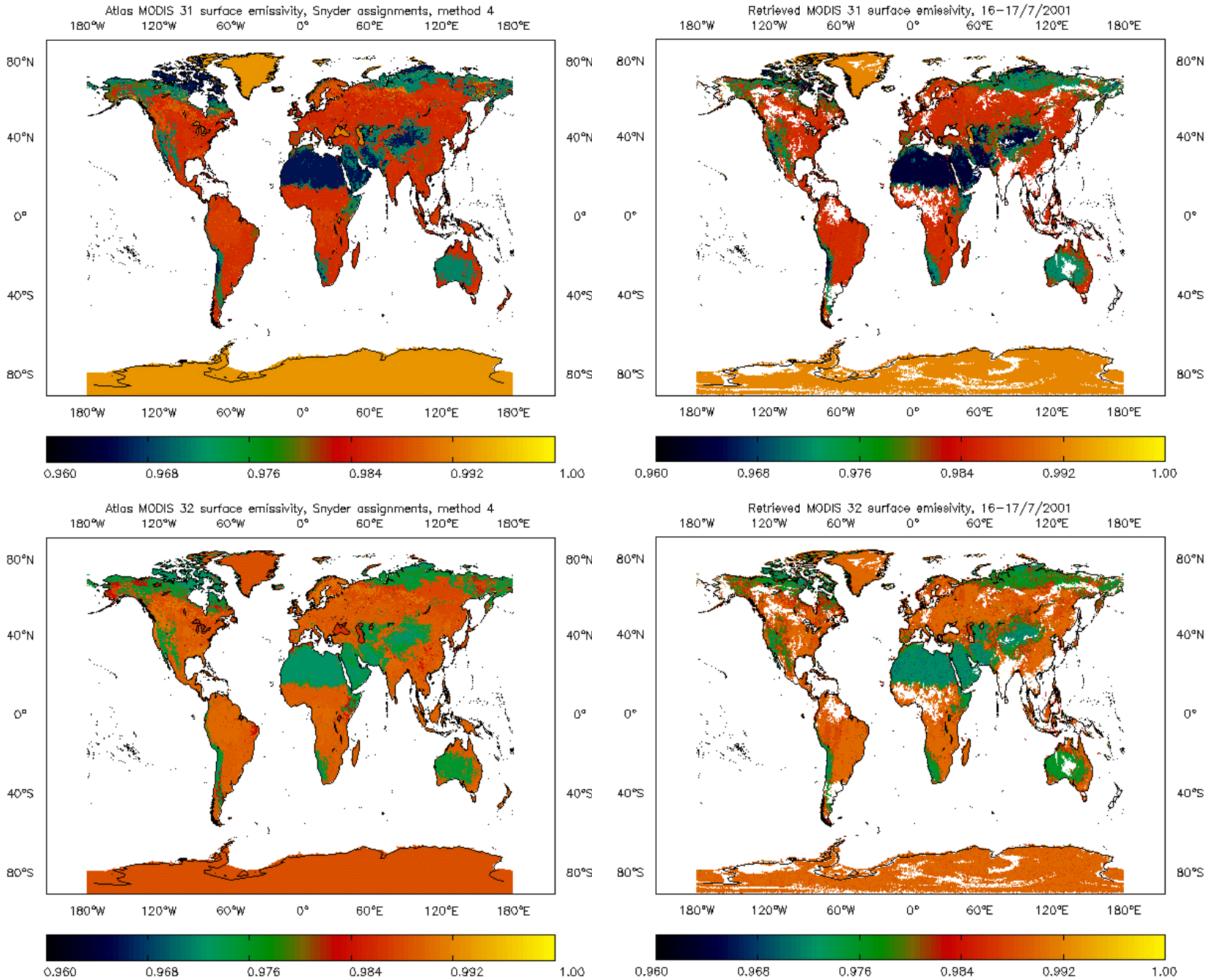
Atlas MODIS 31 surface emissivity, Snyder assignments, method 4
Retrieved MODIS 31 surface emissivity, 16-17/7/2001
Atlas MODIS 32 surface emissivity, Snyder assignments, method 4
Retrieved MODIS 32 surface emissivity, 16-17/7/2001
180°W
120°W
60°W
0°
60°E
120°E
180°E
80°N
40°N
0°
40°S
80°S
0.960
0.968
0.976
0.984
0.992
1.00

Figure 29: Comparison between band 31 (11.0 μm) and band 32 (12.0 μm) land surface emissivity values for July predicted by the tuned scheme described in the text (Method 4) with MOD11_L2 data from 16 - 17/7/2001.

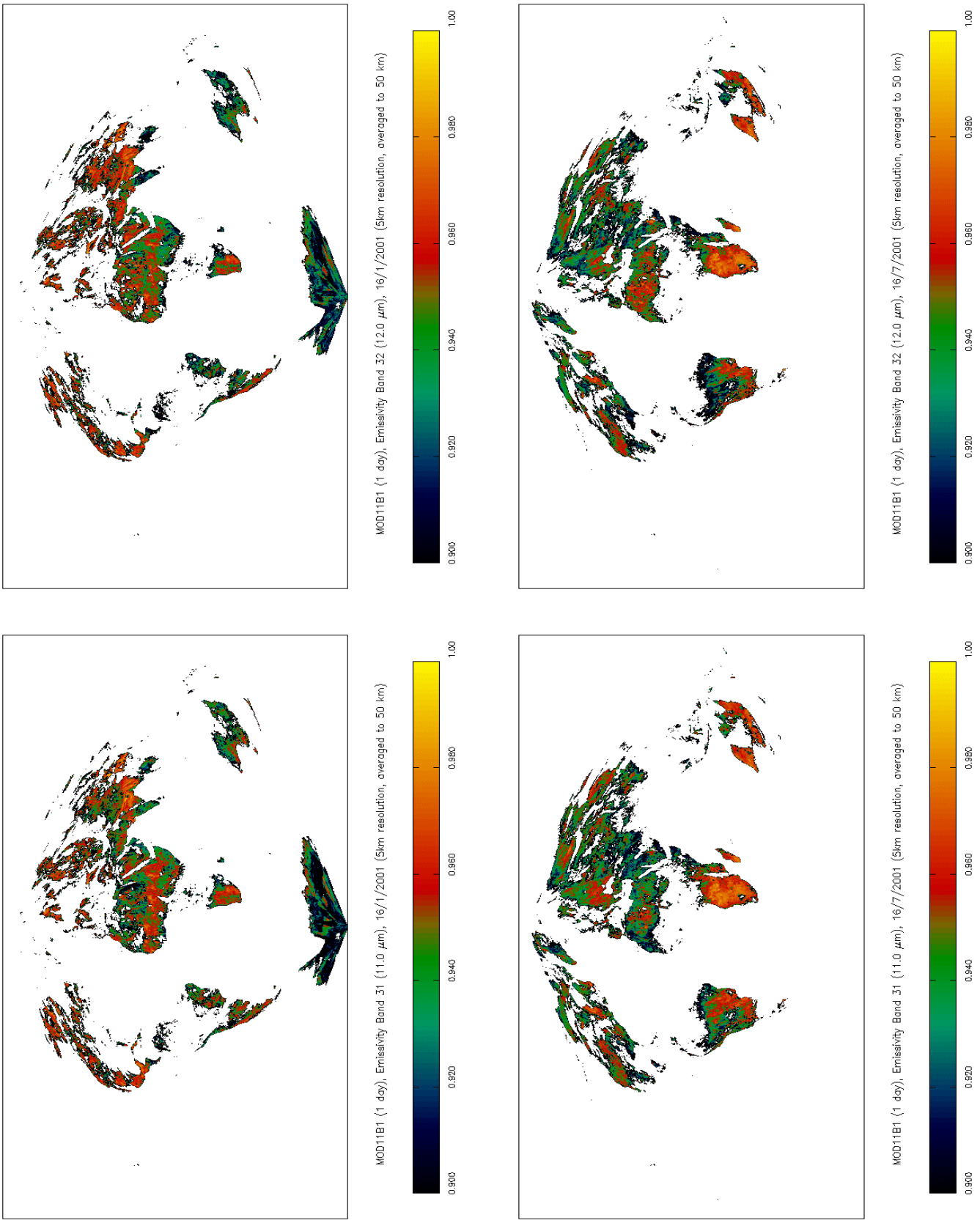

Figure 30: Surface emissivity data from the MODIS day/night product (MOD11B1) for band 31 (11.0 μm) and band 32 (12.0 μm) on 16/1/2001 and 16/7/2001.